Photonic crystal fibres for chemical sensing and photochemistry

Post-print of a peer-reviewed article published by the Royal Society of Chemistry.
Published article available at: http://dx.doi.org/10.1039/C3CS60128E

Cite as:
Cubillas, A. M., Unterkofler, S., Euser, T. G., Etzold, B. J. M., Jones, A. C., Sadler, P. J., Wasserscheid, P., & Russell, P. S. (2013). Photonic crystal fibres for chemical sensing and photochemistry. *Chemical Society Reviews*, 42(22), 8629-8648.

Manuscript received: 05/04/2013; Article published: 11/06/2013

Photonic crystal fibres for chemical sensing and photochemistry**

Ana M. Cubillas,[1,2] Sarah Unterkofler,[1] Tijmen G. Euser,[1] Bastian J. M. Etzold,[2,3] Anita C. Jones,[4] Peter J. Sadler,[5] Peter Wasserscheid[2,3] and Philip St.J. Russell[1,2,6,*]

[1]Max Planck Institute for the Science of Light, Guenther-Scharowsky-Str. 1/Bldg. 24, 91058 Erlangen, Germany.

[2]Cluster of Excellence 'Engineering of Advanced Materials', Friedrich-Alexander-Universität Erlangen-Nürnberg, 91058 Erlangen, Germany.

[3]Lehrstuhl für Chemische Reaktionstechnik, Friedrich-Alexander-Universität Erlangen-Nürnberg, 91058 Erlangen, Germany.

[4]EaStCHEM, School of Chemistry, Joseph Black Building, University of Edinburgh, West Mains Road, Edinburgh, EH9 3JJ, UK.

[5]Department of Chemistry, University of Warwick, CV4 7AL Coventry, UK.

[6]Department of Physics, Friedrich-Alexander-Universität Erlangen-Nürnberg, 91052 Erlangen, Germany.

[*]Corresponding author; e-mail: philip.russell@mpl.mpg.de, fax: +49 9131 6877 309, tel: +49 9131 6877 301

[**]The authors gratefully acknowledge the funding of the Koerber foundation, the European Research Council (grant no 247450 for PJS), and the German Research Council (DFG) which, within the framework of its 'Excellence Initiative', supports the Cluster of Excellence 'Engineering of Advanced Materials' (www.eam.uni-erlangen.de) at the University of Erlangen-Nuremberg. The authors are also grateful to Jocelyn S. Y. Chen, Nicola J. Farrer, Ruth J. McQuitty, Silke Rammler, Michael Scharrer, Matthias Schmidt, Nicola Taccardi and Gareth O. S. Williams for collaboration.

Graphical abstract:

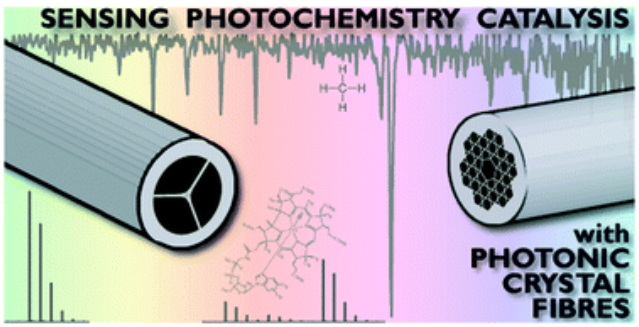

Abstract

In this review, we introduce photonic crystal fibre as a novel optofluidic microdevice that can be employed as both a versatile chemical sensor and a highly efficient microreactor. We demonstrate that it provides an excellent platform in which light and chemical samples can strongly interact for quantitative spectroscopic analysis or photoactivation purposes. The use of photonic crystal fibre in photochemistry and sensing is discussed and recent results on gas and liquid sensing as well as on photochemical and catalytic reactions are reviewed. These developments demonstrate that the tight light confinement, enhanced light-matter interaction and reduced sample volume offered by photonic crystal fibre make it useful in a wide range of chemical applications.

1. Introduction

Optical fibre technology has been extensively developed in the past decades mainly as a result of its use in optical telecommunications. High performance and low cost optical fibre components are available, motivating the use of fibres in other research areas such as sensing and detection.[1] Examples of fibre sensors can be widely found for chemical,[2,3] biological,[4,5] biomedical,[6,7] and environmental[8,9] applications. Besides extremely low attenuation, optical fibres offer many advantages over conventional electronic sensors, such as immunity from electromagnetic interference, compact size, light weight and possibility of remote and distributed measurements.[1]

Conventional optical fibres usually consist of a germanium-doped silica core surrounded by a pure silica cladding with slightly lower refractive index. For sensing, an important limitation of conventional fibres is that cumbersome post-processing techniques are required to allow the guided light to interact with a sample. Typically, this is done by partially removing the cladding by chemicaletching,[10] polishing,[11,12] tapering[13] or by flame exposure.[14] As these processes damage the fibre to some extent, the resulting devices are fragile and require additional packaging. Furthermore, the interaction with chemical samples can be achieved only *via* evanescent wave penetration and is, therefore, rather weak.[15]

The overlap between sample and light can potentially be much improved by loading chemicals into a hollow capillary. This works, however, only if the refractive index of the chemical solution is higher than that of the glass, permitting total internal reflection to operate. Even then the resulting waveguide is typically multimode, making precise photochemical measurements very difficult. If the refractive index of the liquid is lower than that of the glass (such as is the case in aqueous solutions) light confinement is very leaky, the waveguiding highly lossy and the path-length is limited to a few cm at most.[16,17]

A possible way to improve the guidance properties of hollow waveguides is to surround them with a radially periodic cladding of concentric high and low-index layers. Appropriately designed, this cladding structure acts

as an omnidirectional mirror that allows light guidance in a low-index hollow core. The main application of these so-called *Bragg fibres*[18] is delivery of high-power laser pulses, but recently liquid-phase[19] and gas sensing applications[20] have also been demonstrated. A similar guidance mechanism is used in on-chip liquid-core antiresonant reflecting optical waveguides (ARROWs).[21,22] The limitation of both approaches lies in the complex fabrication process, which involves multiple material deposition steps, resulting in imperfections that ultimately limit the transmission as well as the level of light confinement that can be achieved.[18–24]

In 1996 a major breakthrough in optical fibre technology came with the advent of photonic crystal fibre (PCF), a novel structure that has unique properties not achievable with any other fibre.[25,26]The initial motivation for developing PCFs was to trap light in a hollow air core by surrounding it with a 2D periodic 'photonic crystal'[27,28] cladding consisting of microscopic hollow capillaries running along the entire length of the glass fibre.[29] The design of this cladding allows accurate tuning of the waveguiding properties of the PCF.[26] In particular, it has resulted in technological milestones such as the first demonstration of low-loss guidance of light in a hollow core,[30,31] and fibres that guide only the fundamental mode at all frequencies: 'endlessly single mode' PCF.[32]

An important advantage of PCFs over conventional optical fibres is that the hollow channels allow infiltration of chemical samples. This allows them to be probed by the guided light, resulting in fibre-based optofluidic[33–35] devices. The low transmission loss allows samples to interact strongly with guided light over very long path-lengths, making PCF an excellent candidate for sensing and photochemical applications.

In this review paper we introduce PCFs as novel miniaturised chemical sensors and photochemical reactors. The first chapter is an overview of the different types of PCFs available and their interactions with chemical samples. We then review the different possibilities for introducing liquid chemical samples in the channels of the fibre and also provide a figure of merit for light-matter interactions. Finally, we discuss some of the recent applications of PCFs in chemical sensing (Chapter 2) and photochemistry (Chapter 3).

1.1 Types of PCF

The fabrication of PCF is based on the so-called 'stack-and-draw' method, in which glass capillaries are stacked into a macroscopic version of the geometry desired in the fibre.[25] Lattice defects (such as the core region) can be created by adding glass rods (solid-core PCF) or by leaving out several capillaries (hollow-core PCF). An overview of different types of PCF that have been experimentally realised is shown in Figure 1. This section discusses various types of PCFs and their application to chemistry.

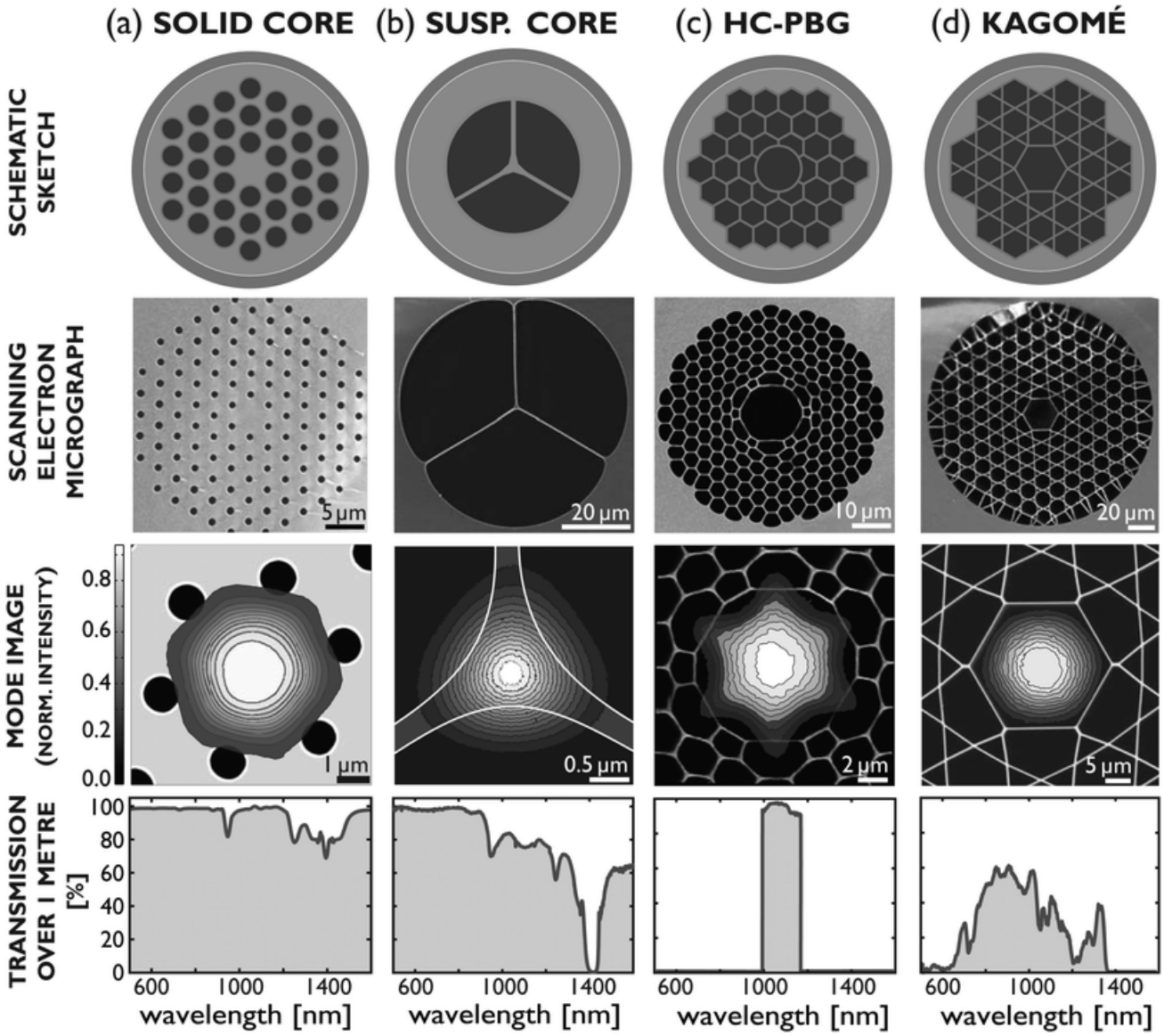

Figure 1. From top to bottom: schematic sketch of the PCF geometry; scanning electron micrograph(SEM) of the core and surrounding cladding; measured fundamental optical mode guided in the core of the fibre (solid white lines show the boundaries of the silica microstructure and dark is air); and transmission over one metre of fibre for (a) a SC-PCF; (b) a suspended-core PCF; (c) a HC-PBGF and (d) a kagomé HC-PCF.

1.1.1 Solid-core PCFs (surface sensitive spectroscopy). Solid-core PCF (SC-PCF) consists of a glass core surrounded by a periodic array of cladding channels, as illustrated in Figure 1(a). The guidance mechanism in such fibres is total internal reflection, similar to telecom optical fibres.[25] In SC-PCF the hollow channels reduce the effective refractive index of the cladding below that of the core. In addition, the dispersion of the guided modes is strongly influenced by the microstructured cladding.[32,36] The large degree of freedom in the design of the SC-PCF microstructure uniquely allows properties such as endlessly single mode (ESM) behaviour,[32] large mode areas,[37] high birefringence,[38] high nonlinearity[39] and exceptional control of

dispersion.[40] At the same time, advances in fabrication techniques have strongly reduced transmission losses of SC-PCF, in the best case down to values comparable to those in standard telecommunication fibres (0.18 dB km^{-1} at 1550 nm).[41] A combination of ESM behaviour and precise dispersion tailoring has allowed the generation of supercontinua that can span ultrabroad wavelength ranges (400–2400 nm) while offering spectral densities several orders of magnitude higher (mW nm^{-1}) than with conventional white-light sources.[42] Such single-mode *supercontinuum* sources are currently widely used in sensing[43–45] and in optical coherence tomography.[46–48]

In sensing applications of SC-PCF, light guided in the solid core interacts with samples *via* a weak evanescent field penetrating the surrounding cladding.[49,50] A major advantage over evanescent field sensing techniques based on conventional fibres[10–14] is that the sample can simply be pumped into the cladding holes, without the need for cumbersome post-processing techniques. The degree of evanescent field penetration into the cladding holes of SC-PCF can be controlled *via* parameters such as core size, hole diameter and pitch (the distance between the hollow channels).[50] In this way, optical overlaps (*i.e.* fraction of optical power that interacts with infiltrated samples in the cladding channels) as high as 5% have been achieved.[49] The fibre geometry allows the use of long interaction lengths which compensate for the relatively low light-sample overlap. Early examples of absorption spectroscopy using SC-PCFs include biomolecule,[51,52] gas[53] and liquid sensors.[54] Another approach is the inscription of long period gratings (LPGs) in the core of SC-PCFs using CO_2 laser post-processing techniques. The sharp optical resonance of such gratings strongly depends on the refractive index of the surrounding media. This type of sensor has allowed, for instance, the detection of label-free biomolecules immobilised on the walls of the cladding holes.[55]

An important limitation of SC-PCF is the large flow resistance in the micron-scale cladding holes. Various techniques have been developed to accelerate the exchange of samples, for instance by using laser-machining to create side-access holes at specific locations along the fibre.[56–61] A more elegant approach is based on a relatively simple suspended-core PCF design, consisting of a solid core held in air by three silica nanowebs (Figure 1(b)).[62,63] The sample can simply be pumped in *via* the three large cladding holes. The fraction of evanescent field that extends into the filled cladding holes can be tuned by varying the core diameter, and overlaps up to 30% are feasible for very small cores.[64] Due to the evanescent wave sensing mechanism, these fibres are ideal for broadband transmission and detection of surface-bound analytes.[64–66]

1.1.2 Hollow-core PCFs (bulk sensitive spectroscopy). The development of hollow-core photonic crystal fibre (HC-PCF) represents a breakthrough in optical fibre technology, uniquely allowing tight light confinement and low-loss guidance in a core whose refractive index is less than that of the glass. The first type of HC-PCF, known as hollow-core photonic bandgap fibre (HC-PBGF) (Figure 1(c)), consists of a central hollow core (typical diameters 5 to 30 μm), surrounded by a honeycomb lattice of hollow channels.[30,67]

The periodic cladding acts as a highly reflective mirror that prevents light from escaping the hollow core; it possesses a photonic bandgap.[30,67] As a result, low-loss guided modes form within certain wavelength ranges where a core resonance coincides with a photonic bandgap. In contrast to other hollow waveguides, HC-PBGF can provide extremely low transmission losses, as low as 1.2 dB km^{-1}.[31,68,69] In addition to the low loss, the optical modes in HC-PBGF are insensitive to fibre bends, allowing flexible fibre pathways. While the typical transmission window of HC-PBGF is a few hundred nanometres wide, its centre position can be shifted over a wide range by up- or down-scaling the PCF design, and it can even provide quite low attenuation at wavelengths where the glass absorption is high, such as in the infrared.[70,71] Low transmission losses and a tunable transmission window make HC-PBGF highly suitable for sensitive narrow-band gas-phase sensing applications.[72–76]

The second type of HC-PCF, kagomé HC-PCF, is named after its particular lattice arrangement in the cladding structure (Figure 1(d)). In contrast to HC-PBGF, this fibre does not possess any bandgaps in the cladding, leading to increased transmission losses of the order of 1 dB m^{-1}.[77–79] Recent reports, however, have shown that losses in kagomé HC-PCF can be reduced to below 100 dB km^{-1} by varying the design of the core surround.[80,81] The most important property of kagomé HC-PCF is that it allows transmission windows that extend over very broad wavelength ranges, spanning from the UV to the near-infrared (NIR). This fibre is therefore the preferred choice for broadband spectral measurements such as liquid-phase experiments on sub-μL sample volumes.[82–85]

1.2 Liquid filling of PCFs

To use PCFs in sensing and photochemistry experiments on liquid-samples, the sample must be pumped into the holes of the fibre. Figure 2(a) shows a schematic of a typical experimental set-up, valid for most of the experiments discussed in this review paper. Liquid-filling is established by inserting a piece of PCF into small pressurisable cells equipped with HPLC tubing connectors and optical access windows. Cells are typically custom-made from metal or plastic and can be fabricated with a dead volume of around 50 μL, see Figure 2(b). Although this is sufficiently small for measurements on static samples, it can introduce inconveniently long dead times in continuous-flow experiments. We have therefore recently constructed and custom-built a true optofluidic interface based on an off-the-shelf microfluidic chip.[84] This contains a simple straight channel with two inlet ports open towards one side of the chip, see Figure 2(c). The *perpendicular* arrangement of channel and fibre axis allows in-coupling to be established through the thin polymer layer at the covered side of the chip. The total dead volume of this optofluidic interface is less than 1 μL.

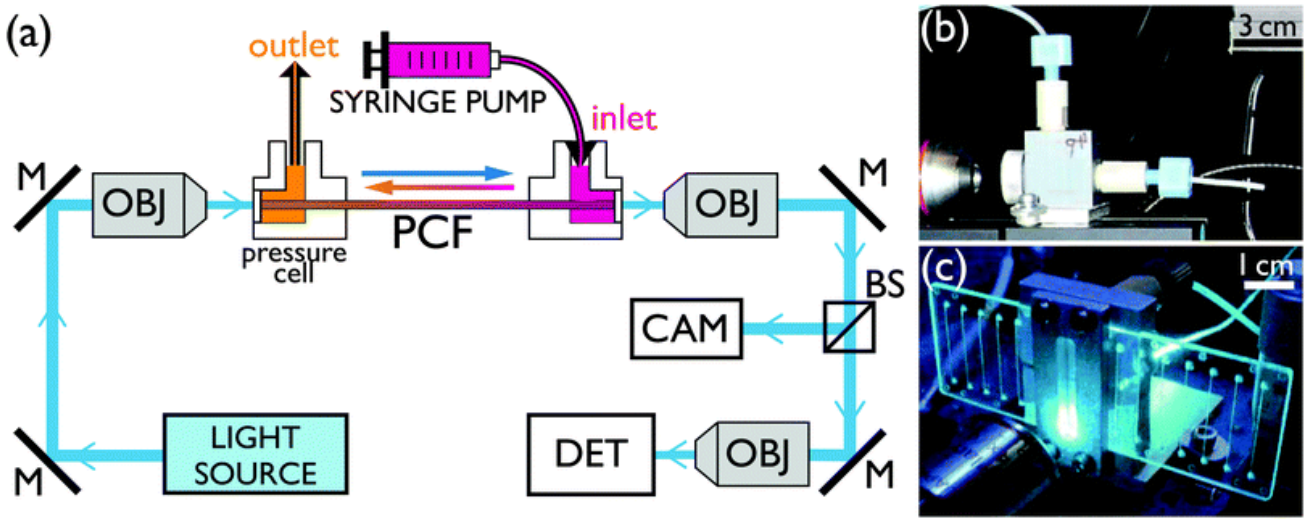

Figure 2. (a) Schematic drawing of a typical set-up for in-fibre sensing and photochemistry. The PCF is mounted into pressure cells, its end facets being optically accessible *via* thin windows. Light is coupled into the core using a microscope objective lens (OBJ) with matching numerical aperture. The fibre is either filled or a continuous flow established *via* pressurisation with a syringe pump. The out-coupled light is monitored with a camera (CAM), to analyse the transmitted optical mode, and a detector (DET), such as a power meter or a spectrometer. M: mirror, BS: beam splitter. (b) Photograph of a custom-made plastic pressure cell. (c) Photograph of an optofluidic chip-to-fibre mount for continuous flow experiments.

There are two different ways to achieve light-guidance in liquid-filled HC-PCF, depending on how the structure is initially filled.

1.2.1 Selective core filling. The first approach is based on selectively filling the core of a HC-PCF with liquid, while leaving the cladding holes air-filled.[49,86,87] In this case, the refractive index of the core exceeds the average refractive index of the fibre cladding, creating a total internal reflection waveguide. The procedures required to fill the core selectively are somewhat cumbersome. In one report the cladding holes are blocked with UV-curable adhesive using a multi-stage fabrication procedure.[88] In a second approach, the cladding holes are thermally collapsed by a fusion splicer to prevent them from being filled.[87,89] In both cases, the resulting waveguide is broadband guiding. However, due to the large refractive index step between liquid core and air-filled cladding, and the large core diameter, such fibres typically support many optical modes, whose mutual interference causes intensity fluctuations that make accurate spectroscopic experiments challenging.

1.2.2 Complete filling of the PCF structure. A second approach is based on preserving the photonic bandgap guidance of HC-PBGF after liquid-filling. This is possible when the entire holey structure is homogeneously filled up along its length with a filling medium whose refractive index is lower than that of the glass.[90–92] Upon liquid-filling, a guidance band located around wavelength λ in an unfilled fibre, will shift to a shorter wavelength λ_{fill}. This behavior is well-approximated by a scaling factor that depends on the refractive indices of the liquid (n_{fill}) and the glass (n_{silica}):

$$\lambda_{fill} = \lambda \sqrt{\frac{n_{silica}^{\ 2} - n_{fill}^{\ 2}}{n_{silica}^{\ 2} - 1}}$$

For a water-filled PCF the square root factor in eqn (1) is ~0.57.†

The validity of the index scaling law is demonstrated in Figure 3, where the transmission properties of a water-filled and an air-filled HC-PBGF are compared. In the 800–900 nm range, light is guided in a single optical mode in the water-filled fibre (Figure 3(b)) and the loss is dominated by the intrinsic absorption of the water[93] (orange dashed curve, Figure 3(a)), indicating that the HC-PBGF does not add a significant waveguide loss. The wavelength of the guidance band in the water-filled fibre (turquoise, Figure 3(a)) compared to the air-filled fibre (black) is shifted in excellent agreement with the scaling factor of 0.556 predicted by eqn (1).

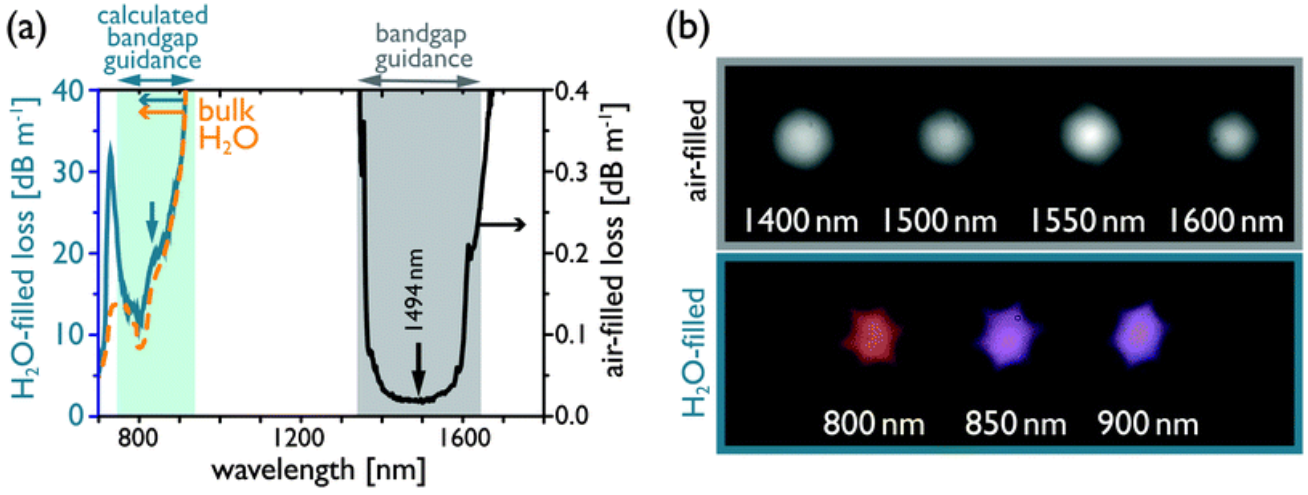

Figure 3. (a) Air- (black) and water-filled (turquoise) loss spectra of a HC-PBGF. The loss of bulkH_2O is plotted in orange. (b) Core modes present in the wavelength ranges corresponding to the transmission bands of air- and water-filled fibre.

1.3 Sample exchange in PCF

Residual contamination from a previous sample could become a practical limitation when using PCF in liquid-phase experiments. In principle, analytes can readily be removed by continuous flow washing with a suitable cleaning agent. For efficient removal of residual analyte, the cleaning agent should interact with the analyte more strongly than the fibre walls. For highly polar analytes that strongly interact with the walls, removal by flow washing may not be possible. In this case, it may be feasible to prevent surface adsorption by derivatising the walls, *e.g.* by applying an internal hydrophobic silanelayer.[94,95] It must be noted that in the case of HC-PCF, in which molecules are excited away from the surface, the effect of surface adsorption is much less critical than in SC-PCF, in which molecules in close proximity to the surface of the solid core are excited.

1.4 Figure of merit for light-matter interactions

In case of photochemical reactions, two important parameters determine the effectiveness of the experiment. Firstly, the effective path length L_{eff} of the probe light (defined as the length at which the intensity drops to $1/e$ of the initial value in the pure liquid host, that is, in the absence of any chemical sample) should be long enough to allow detection of low concentrations. Secondly, the cross-sectional area of the sample cell A_{eff} should be as small as possible, so as to maximise the intensity of the optical pump field, in particular for reactions with low quantum yields.

In order to quantify the performance of HC-PCF in comparison to other systems, a useful figure of merit for light-matter interactions was proposed by Benabid *et al.*:[77]

$$f_{\text{om}} = \frac{L_{\text{eff}}\lambda}{A_{\text{eff}}}$$

The figure of merit (f_{om}) is evaluated for three different systems: firstly, as a reference, we consider the situation of a laser beam focused into a standard cuvette (1 cm^2 square cross-section with an optical path length of 1 cm). Since molecules can freely diffuse in and out of the irradiated volume, the effective cross sectional area of a cuvette is 1 cm^2, regardless of how tightly the beam is focused.[82]The figure of merit can be increased by a factor of 100 by reducing the cross-section of the cuvette to 1 mm × 1 mm, which is close to the smallest practical cuvette size. Secondly, thin hollow capillary waveguides could be used to further decrease the cross-section A_{eff}. In this case, the $1/e$ decay length of the fundamental guided mode in a straight capillary of bore radius r is given by:

$$L_{\text{eff}} = 6.83\frac{r^3}{\lambda^2}\frac{\sqrt{v^2-1}}{(v^2+1)}$$

where $v = n_2/n_1$, n_1 and n_2 being the refractive indices in the bore and the glass.[96] This means that the effective length decreases with the cube of the bore radius. Finally, the performance of liquid-filled HC-PCFs is evaluated for different values of fibre loss.

The figure of merit for the various systems at a wavelength of 532 nm is plotted as a function of core diameter in Figure 4. It becomes clear that a hollow capillary waveguide represents a big improvement compared to cuvette-based approaches. Nevertheless, it is worth noting that losses in hollow capillary waveguides are extremely sensitive to bending, making the use of longer capillaries very difficult. HC-PCFs, on the other hand, are almost completely insensitive to bend losses and therefore uniquely combine long interaction lengths with tightly confined light.[97,98] Due to low transmission losses, HC-PCF offers seven orders of magnitude improvement over a standard cuvette, and two orders of magnitude over a hollow capillary of the same core size. Experimentally, realistic loss values at 532 nm for a liquid-filled HC-PCF with a core diameter of 24 μm are of the order of 2 dB m^{-1}, resulting in a figure of merit that is three orders of magnitude higher than for a capillary with similar dimensions, and more than eight orders better than a standard cuvette.

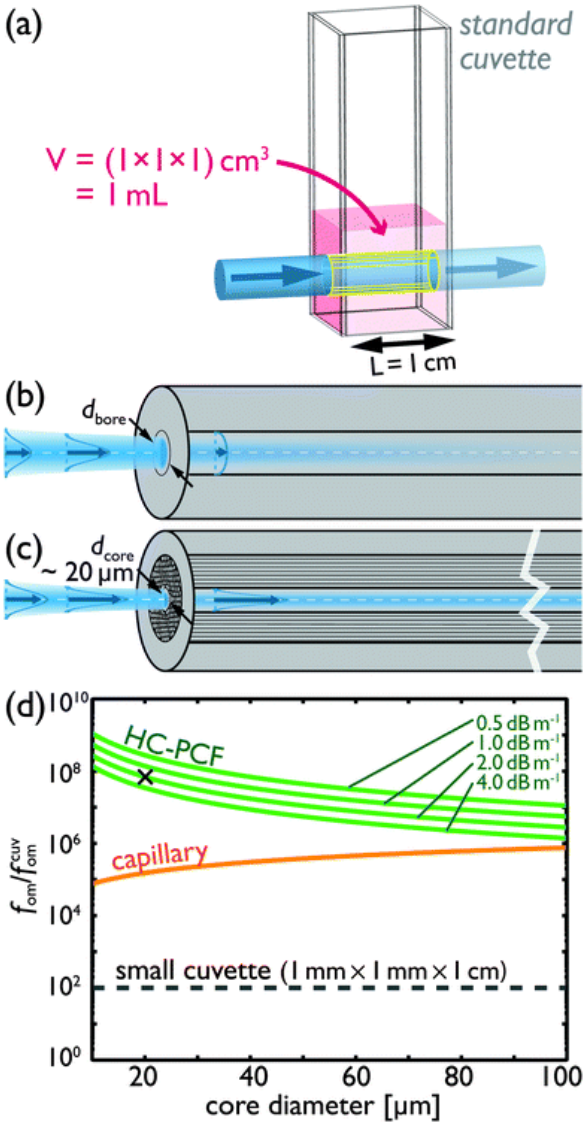

← ***Figure 4.*** Comparison of three different liquid sample cell geometries. (a) Standard cuvette, (b) capillary waveguide, and (c) HC-PCF. (d) Figure of merit for light-matter interactions, relative to that of a 1 cm × 1 cm standard cuvette. f_{om} is evaluated for a reduced size cuvette, a liquid-filled capillary, and a liquid-filled HC-PCF for a range of loss values. The cross indicates the experimental value for a liquid-filled kagomé PCF.

2. Sensing and detection in PCFs

The use of PCF in optical sensing has generated much interest,[75] in particular because the fibre microstructure obviates the need for complex post-processing. Furthermore, it allows the sample volume to be strongly reduced while providing the robustness and flexibility required for fibre sensors. For absorption-based sensors, HC-PCF maximises light-matter interactions over much longer path-lengths than in conventional sample cells, offering an ideal environment for optical spectroscopy. Interestingly, the different types of PCF available allow the probing both of bulk solution samples, as in HC-PCF, and of molecules close to the internal fibre surfaces (SC-PCF).

Practical applications of PCF-based chemical sensors will be discussed in the following sections, specifically narrow-band gas sensing measurements, broadband liquid-based chemical sensors andfluorescence detection.

2.1 Gas sensing in PCFs

Increasing environmental awareness and the resulting strict emission standards have resulted in a strong demand for high performance sensing and monitoring systems for trace gases.[1,99–101] High sensitivity gas detectors are also essential for many industrial processes,[102,103] safety[104,105] and biomedical[106,107] applications. What makes this a challenge is that most gases of interest have their strongest molecular absorption lines in the mid-infrared (MIR) region, where optical components are expensive and cumbersome to operate.[108] To allow gas detection at shorter wavelengths, measurement schemes often probe molecular transitions related to harmonic or combination bands. These transitions lie in the NIR, where high-quality and relatively inexpensive optical telecom lasers and detectors are readily available. Unfortunately, the NIR absorption lines are typically very weak, limiting the detection sensitivity. To enhance the interaction length, and thus the sensitivity, conventional techniques make use of multi-pass cavities (such as Herriot[109,110] or White[111] cells). However, these gas cells are bulky, require large gas volumes and are prone to misalignment.

Offering extremely small sample volumes, low transmission losses and high flexibility, PCF is an attractive alternative to conventional gas cells. Gas samples can be flowed into the micron-sized hollow channels, allowing them to interact with the guided optical modes. The first experiments on PCF-based gas detectors made use of evanescent wave sensing in SC-PCF.[49,53,63,112–115] Due to the relatively low overlap between gas sample and light in this type of fibre, the sensitivity achieved was very low.

A much higher overlap, typically more than 95%, is achieved in HC-PCF.[30] In pioneering experiments, Ritari *et al.* showed detection of gases in HC-PCF by direct absorption spectroscopy in the NIR.[72] Using similar techniques, HC-PCFs have since been used in sensing experiments on acetylene (C_2H_2)[116] and ammonia (NH_3) at 1.5 μm,[117] methane (CH_4) both at 1.3 μm[118] and 1.6 μm[73] in the NIR and 3.3 μm[74,119] in the MIR, ethylene (C_2H_4)[120] and ethane (C_2H_4) at 1.6 μm[121] or carbon dioxide (CO_2) at 2 μm.[122] In each case, the HC-PCF design

was adjusted to provide optical guidance in the wavelength range of interest. HC-PBGF has also been used in combination with more complex spectroscopic techniques to increase the sensitivity of the system. Recent demonstrations include wavelength[123] and frequency modulation,[124] correlation[125] and cavity ring-down spectroscopy.[126]

As an example, Figure 5 shows direct methane absorption spectra in the NIR region using HC-PBGFs with transmission bandgaps in the $v_2 + 2v_3$ at 1.3 μm[118] (a) and in the $2v_3$ band at 1.6 μm[73] (b). The estimated detection limits are as low as 98 parts per million volume (ppmv) in the first case[127] and 10 ppmv in the second.[73] The latter value corresponds to a minimum detectable absorbance (MDA) of 8×10^{-4}, similar to typical values achieved using direct absorption spectroscopy.[128] Remarkably, despite long path-lengths of several metres, the sample volume was below 6 μL in the core of the fibre (around 3.22×10^{17} gas molecules).

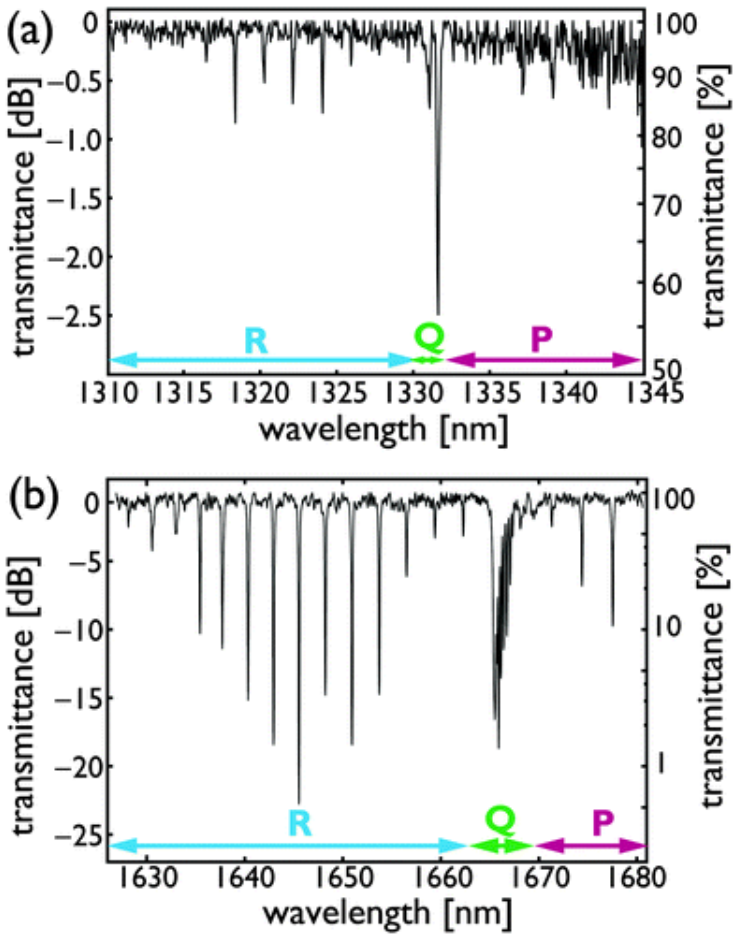

Figure 5. Transmission spectrum of methane measured at room temperature, a relative pressure of 1 atm and a methane concentration of 18 750 ppmv in air (a) at the combination band $v_2 + 2v_3$ at 1.3 μm using a 560 cm-long HC-PBGF,[118] and (b) at the overtone band $2v_3$ at 1.6 μm using a 510 cm-long HC-PBGF.[73] R, P and Q branches are labelled.

An important challenge in PCF gas detection is to achieve a sufficiently fast response time. Filling by free diffusion of gas into the holes of the PCF can take several hours for fibre lengths of several metres.[116,129] The response can be reduced to several minutes by use of vacuum[72] or pressure-assisted[130] filling methods. Recently it has been shown that transverse side access holes can be made in the PCF cladding, allowing gas to reach the hollow-core.[131] Typical techniques are focused ion beam (FIB) processing,[56] hole blowing[57] or fs-laser hole drilling.[60,61] Additional optical transmission losses can be reduced to below 0.1 dB per drilled hole,[120] while the response time of the sensor can be reduced to 3 s.[132] Another approach involves splitting the PCF into shorter, butt-coupled pieces,[133] which can also reduce the diffusion time to minutes.

Finally, gas-filled hollow-core PCFs have been widely investigated in a range of applications such as high-resolution saturation spectroscopy,[124,134,135] wavelength references,[136] and nonlinear quantum optics.[137] It must also be noted that the main field of application of gas-filled PCFs is nonlinear spectroscopic experiments, in which PCFs have allowed to explore new regimes of light-matter interaction. Comprehensive reviews of nonlinear optics experiments in gas-filled HC-PCF have recently been written by Bhagwat and Gaeta[138] and Travers *et al.*[139]

2.2 Liquid sensing in PCFs

There is a large and growing interest in the field of optofluidics[23,33,34,140–142] in which microfluidic circuits[143–145] are combined with integrated optical waveguide structures.[146–148]

Optofluidic sensing applications typically use on-chip waveguides, whose guided modes evanescently interact with collinear microfluidic channels. Due to high losses, interaction lengths are usually limited to a few hundred μm. In order to increase the detection sensitivity, longer path lengths up to several mm have been achieved in planar waveguide geometries[149] and modified conventional fibres.[150]

Much longer path-lengths, up to several metres, have become available with the advent of PCF. Initially, the development of PCF-based evanescent wave sensors advanced the field. In a pioneering experiment, Jensen *et al.* used light guidance in the glass cladding structure of a liquid-filled HC-PCF to detect Cy5-labeled DNA molecules in sub-microlitre volumes of aqueous solution.[151] Soon thereafter, Cordeiro *et al.* presented a SC-PCF with a novel microstructured core design which enhanced the evanescent field overlap with infiltrated liquid samples.[54] Interestingly, the reported absorption spectra of aqueous methylene blue solutions displayed a strongly enhanced P-dimer peak, indicating strong surface adsorption of the molecules on the silica glass. This effect is caused by the high polarity of methylene blue and could potentially be exploited in surface-enhanced sensing applications.

Recently, we have used a one metre long suspended-core fibre for liquid-phase sensing by measuring the broad absorption peak of an aqueous $NiCl_2$ solution.[65] The absence of surface adsorptionallowed a

quantitative analysis of the absorption data. The mode intensity distribution in the fibre was measured and calculated at different wavelengths. At 700 nm, the fraction of light overlapping with the sample was 10%, in good agreement with theory (see Figure 6(a)). The long interaction length in the fibre resulted in a ten-fold enhancement in absorbance (Figure 6(b)). The molar absorptivity spectraobtained from the suspended-core PCF showed quantitative agreement with the reference spectrum measured in a cuvette, even though the sample volume was three orders of magnitude smaller (seeFigure 6(c)).

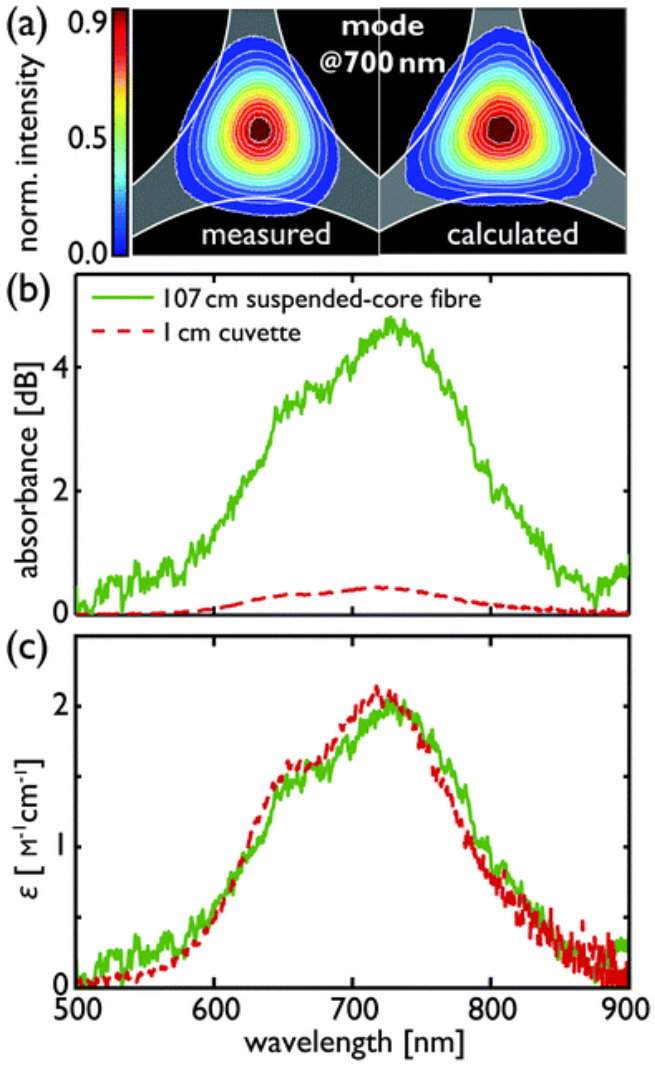

Figure 6. (a) Measured and calculated mode intensity profiles of a water-filled suspended-core fibre at 700 nm wavelength. The relative light sample overlap is 10%. Each square corresponds to 2 × 2 μm^2. (b) Broadband absorption spectra of aqueous $NiCl_2$ solution of concentration 21 mM, measured both in a 107 cm-long piece of fibre (volume 1 μL) and in a 1 cm standard cuvette (volume 1 mL). The absorbance in the fibre is ten times higher than that in the cuvette. (c) Molar absorptivity spectrum obtained by dividing the absorbance data in (b) by the relative power overlap with the sample. The excellent agreement is striking since no parameters were freely adjusted.[65]

2.3 Fluorescence detection in PCF

Due to the high degree of achievable selectivity and sensitivity, possibly even down to the single-molecule level,[152] fluorescence-based sensing has become a widely used methodology in (bio)analytical chemistry. There has been great interest in using PCF for fluorescence studies, where long interaction lengths can be achieved even for very small sample volumes.

In pioneering studies, Konorov *et al.* measured the fluorescence of thiacarbocyanine dye infiltrated into the cladding holes of a HC-PCF. Using a solvent whose refractive index exceeded that of silicaglass (DMSO), an array of fluid waveguide channels was formed, in which light was guided by total internal reflection.[153] In addition, the authors showed a dual cladding SC-PCF design, in which fluorescence molecules are excited by light guided in a central core, while a large-diameter fibre cladding served to collect the fluorescence from the sample.[153]

Employing several novel filling techniques, Cordeiro *et al.* reported fluorescence excitation in a partially filled SC-PCF as well as in a HC-PCF in which the core was selectively filled with rhodaminedye in ethylene glycol.[57] Using a suspended-core PCF made of a high refractive index lead-silicate glass, Ruan *et al.* enhanced the fluorescence detection sensitivity, allowing the detection of quantum-dot labelled proteins down to the 1 nM level.[154] The detection efficiency for fluorescence-based sensing depends on the excitation efficiency as well as the collection efficiency, which both depend on the structural parameters of the fibre such as the core diameter.[64,155] Unfortunately, due to the ill-defined sample illumination conditions in the aforementioned studies, a quantitative analysis was not possible.

The fluorescence detection efficiency can be further improved using a HC-PCF in which the core is selectively filled.[57,156] Smolka *et al.* showed that this system can be used to detect Rhodamine 6G concentrations as small as 100 pM, corresponding to some 120 000 molecules within the sample volume. Nevertheless, since the guidance mechanism is based on total internal reflection, the authors failed to exploit the enhanced guidance characteristics that are made possible through the use of HC-PCF.

We recently reported an improved fluorescence-based scheme using a completely filled kagomé-type HC-PCF.[66] Figure 7(b) shows the resulting fluorescence spectrum of fluorescein solution at an ultra-low concentration of 20 pM, corresponding to 1 000 000 molecules in the core volume of ~90 nL. From the excellent signal-to-noise ratio, we estimate that the detection limit lies 1 to 2 orders of magnitude lower, *i.e.* at 10 000 to 100 000 molecules. The spectrum was also recorded in a suspended-core PCF (Figure 7(c)), using a 15 times higher fluorescein concentration of 300 pM to compensate for the smaller overlap with sample. The similarity of the spectrum measured in the bulk solution, in the HC-PCF, and near the solution–silica interface (SC-PCF) is consistent with previous observations, using conventional evanescent-wave-induced fluorescence spectroscopy, that the spectrum of fluorescein is unperturbed by proximity to the surface.

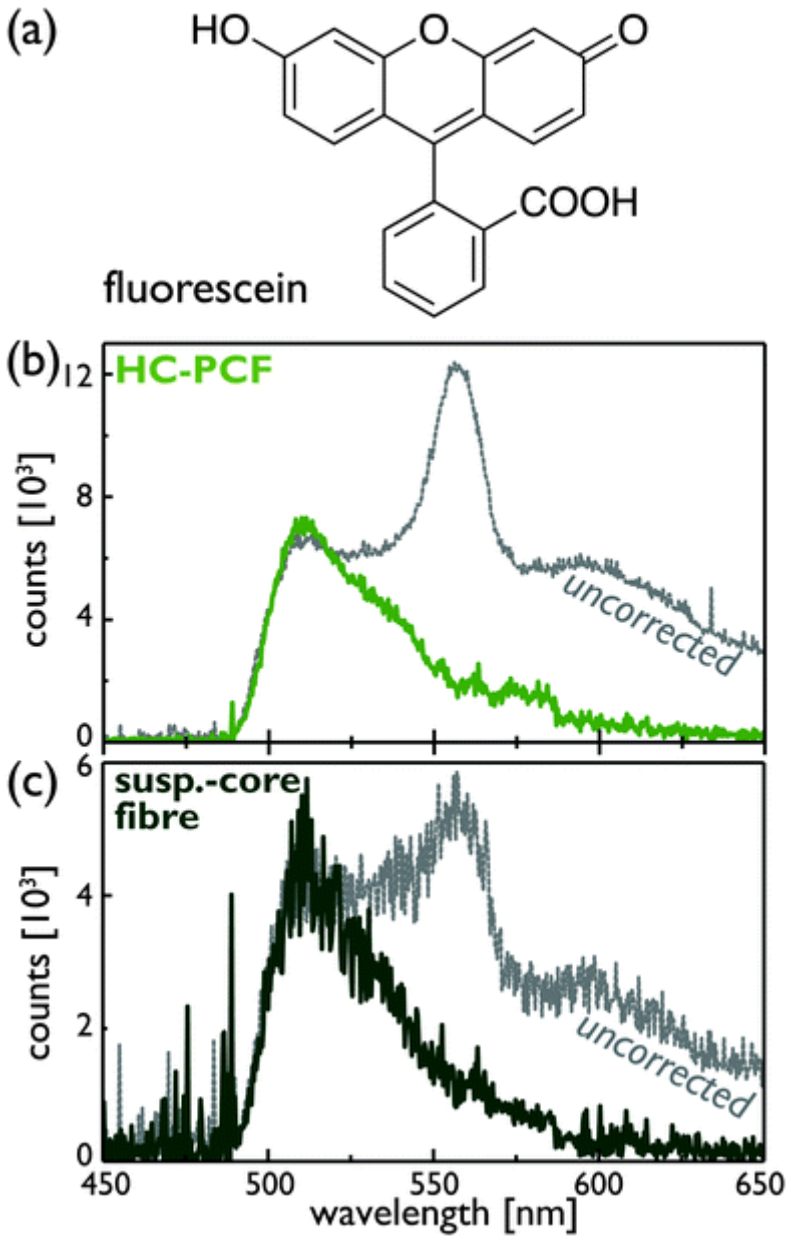

Figure 7. (a) Structural formula of fluorescein. Fluorescence spectra of fluorescein solution (b) in the HC-PCF at a concentration of 20 pM and (c) in the suspended-core fibre at a concentration of 300 pM. In each case, the spectrum is shown before (dotted) and after (solid) subtraction of the water background. The fibre length was 30 cm in each case.[66]

It is well known that the fluorescence lifetime of dyes can depend on the proximity of surfaces. For example, the non-radiative decay rate of rhodamine B depends on the internal rotation of thealkylamino substituents with respect to the planar aromatic ring system,[157] shown in the structural formula in Figure 8(a). Within a bulk solution, the alkylamino groups are free to rotate and are primarily found in a twisted state.‡ Once

adsorbed to a surface, however, the molecules lose their internal rotational freedom, resulting in a lower rate of internal conversion and hence an increased fluorescence lifetime.[158]

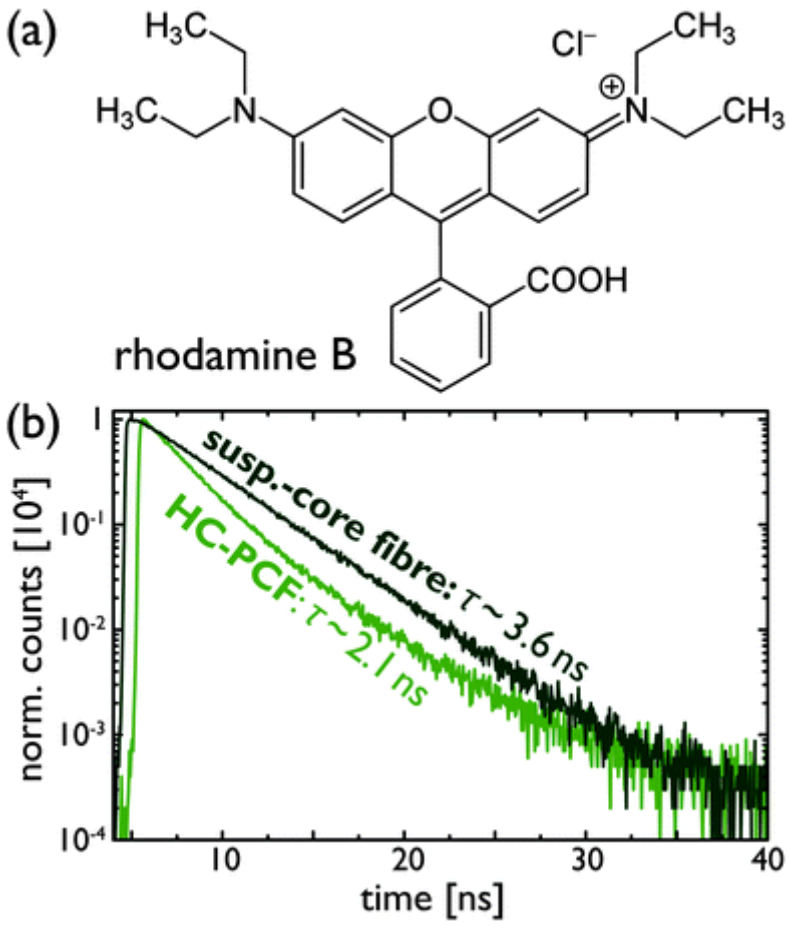

Figure 8. (a) Structural formula of rhodamine B. (b) Fluorescence decays of a 1 nM aqueous solution of rhodamine B in suspended-core fibre and kagomé HC-PCF.[66]

We exploited this effect to investigate the different excitation regimes in the two types of PCF, by comparing fluorescence lifetime measurements of rhodamine B in a HC-PCF with those on a suspended core PCF.[66] The resulting decay curves for a 1 nM solution of rhodamine B are shown in Figure 8(b). In the suspended-core PCF the measured decay is mono-exponential with a lifetime of 3.64 (±0.17) ns. This is in excellent agreement with the lifetime reported previously for rhodamine B adsorbed on colloidal silica[159] and confirms that, in the SC-PCF, molecules at the interface between the solution and the solid core are excited exclusively by the evanescent field. In the HC-PCF a shorter decay time of 2.12 (±0.13) ns is observed, equivalent to that reported for rhodamine B in bulk solution. In fact, this decay shows a slight deviation from mono-exponential behaviour. The quality of the fit is significantly improved by the addition of a second, minor decay component

with a lifetime of 4.0 (±1.4) ns and amplitude of 6%. There is a large uncertainty in the latter lifetime value because of the very small amplitude of this component, but it approximates to that of surface-adsorbedrhodamine B. Thus, there is slight heterogeneity of the emitting population in the HC-PCF; the vast majority (94%) of the fluorophores that are excited are in bulk solution, while only a very small fraction (6%) is subject to surface perturbation, despite the high surface-area-to-volume ratio of the hollow core, which is of the order of 105 m^{-1}. An increase in core diameter would serve to reduce the effect of surface perturbation, but would also reduce guidance efficiency at shorter wavelengths.

3. Photochemistry in PCFs

There is rapid growth in the applications of photochemistry[160] in many areas, including medicine,[161–163] chemical synthesis,[164] the conversion and storage of solar energy[165–169] and data storage.[170]Many of these applications require high pump intensities for rapid photochemical conversion.

The use of HC-PCF for photogeneration and detection of transient species was first reported by Khetani *et al.* using laser flash photolysis.[171] However, the sample solution was excited perpendicular to the fibre core, through the cladding, and monitored by probe light guided along the core. Thus, the path length for the pump beam was extremely short (only a few microns – the diameter of the fibre core) requiring the use of a concentrated (mM) sample solution, and the effective probe path-length was only 1 cm. This study, therefore, failed to exploit the large gain in intensity and sensitivity offered by guidance of both pump and probe beams through the hollow core.

The following sections discuss different schemes for studying photochemical reactions in liquid-filled HC-PCFs that take full advantage of the strong light-matter interaction and detection sensitivity offered. Specifically, recent demonstrations of PCFs as photochemical microreactors in photolysis, isomerisation and catalytic processes will be reviewed.

3.1 Photolysis of cyanocobalamin

As proof-of-principle, the well-known photoaquation[172] of the metal complex vitamin B_{12} (cyanocobalamin, CNCbl) was studied. Cyanocobalamin is a very stable form of vitamin B_{12} and is readily purified and crystallised. For this reason it is produced commercially. It is also approved for medical use and in the body it is converted to active aqua/hydroxo, adenosyl, and methyl cobalamin forms.

In the single-component photolysis reaction, irradiation of aqueous solutions of CNCbl at short wavelengths leads to replacement of the axial CN^- ligand by H_2O, converting CNCbl into $[H_2OCbl]^+$(aquacobalamin or

B_{12b}) (see Scheme 1). The reaction is characterised by a very low quantum yield ($\varphi \sim 10^{-4}$ at pH 6),[172–174] and therefore greatly benefits from the enhanced light intensity in the fibre core of HC-PCFs.

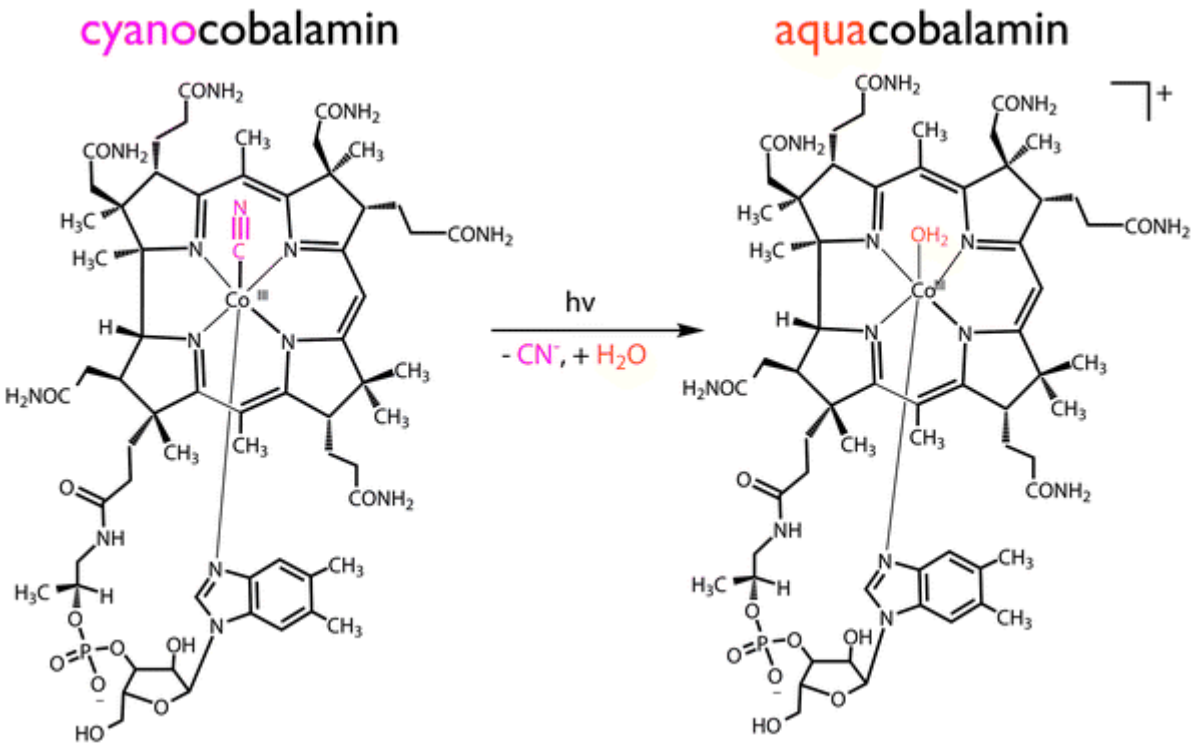

Scheme 1. Photo-induced aquation of cyanocobalamin (CNCbl) to give aquacobalamin, $[H_2OCbl]^+$, in aqueous solution (at low pH). Upon irradiation with blue light, the cyanide ligand is replaced by a water molecule.

The absorption spectra of many cobalamins are highly similar, since the corrin ring is responsible for the dominant spectral features, namely the α and β bands ($\varepsilon \approx 8000–10\,000$ M^{-1} cm^{-1}) in the visible spectral region and the Soret (γ) band ($\varepsilon \approx 25\,000$ M^{-1} cm^{-1}) in the UV region.[172] In the case of photoaquation, exchange of CN^- for H_2O decreases the electron density at the Co^{3+} centre and the α absorption band moves to shorter wavelengths. The reaction was excited by a blue laser beam at a wavelength of 488 nm guided in a liquid-filled HC-PCF. The resulting initial and final absorption spectra are shown in Figure 9(a). The observed shift of the α band towards shorter wavelength is in excellent agreement with previously reported data.

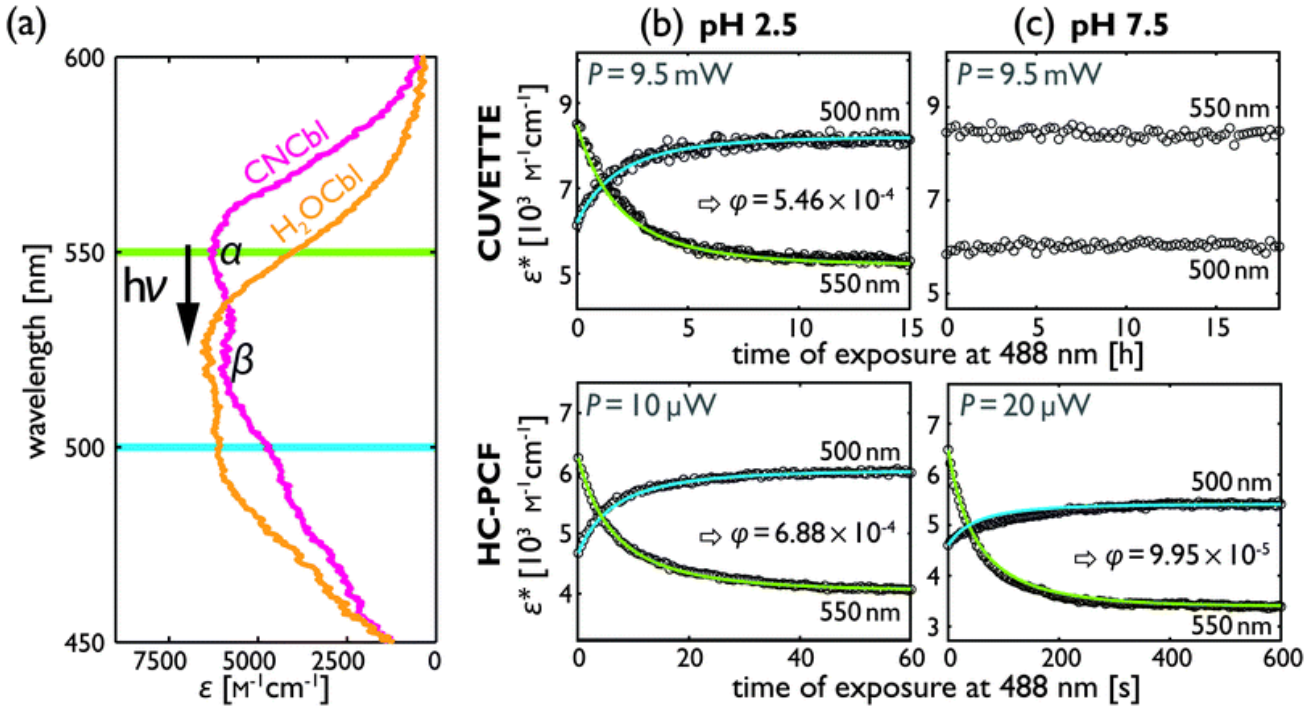

Figure 9. (a) The absorption spectrum of the photoproduct $[H_2OCbl]^+$ (orange) is blue-shifted with respect to CNCbl, the analyte (pink). Temporal monitoring of the photoaquation reaction as performed at (b) low, and (c) high pH values in a cuvette (c = 125 μM) (top) and in a kagomé PCF microreactor (c = 4 μM) (bottom).

The average molar absorptivity $\varepsilon^* = \frac{1}{c_0 L}\int_0^L [\varepsilon_1 c_1(z) + \varepsilon_2 c_2(z)]dz$ of the analyte-product mixture is plotted at two different probing wavelengths, 500 nm and 550 nm, roughly matching the α and β absorption bands. The fits (solid blue and green) were obtained using a reaction kinetics model in which the quantum yield (φ) was the only free parameter.[82]

3.1.1 Absorption spectroscopy and reaction kinetics monitoring of cyanocobalamin photoaquation. It is interesting to compare the dynamics of the photochemical conversion in HC-PCF and cuvette. The rate of photoconversion of CNCbl to $[H_2OCbl]^+$ has previously been shown to depend on the pH of the solution. CNCbl is most stable to photoaquation for pH values between 7 and 8 and converts more rapidly at both the higher and lower extremes of pH.[174] To investigate this effect, the temporal evolution of the absorption at 500 and 550 nm, during photolysis of CNCbl at pH 2.5 and 7.5, was measured both in a cuvette and in a kagomé HC-PCF and is shown in Figure 9(b and c). The cuvette measurements were carried out on 1 mL of 125 μM buffered aqueous CNCbl solution at an excitation power of 9.5 mW. The fibre measurements were performed using a sample volume of ~100 nL (4 μM) and only 10 μW of power at pH 2.5 (Figure 9(b)) and 20 μW at pH 7.5 (Figure 9(c)). The photochemical conversion in the fibre at pH 2.5 occurs within 1 minute, roughly 1000 times faster than in the cuvette, even though the excitation power remains below 20 μW. Previous

studies of the photoaquation of CNCbl required much higher lamp powers (>100 W)[173,174] and/or acidic conditions (pH 4.75).[172]

Strikingly, the strong light confinement in the HC-PCF allowed the reaction to reach completion at pH 7.5 within 10 minutes, using only 20 μW of excitation power. In comparison, no change was observed in the cuvette-based experiment, despite a 500-times-higher optical power and 17 hours-long exposure time (Figure 9(c)). To quantify the effect of pH on the reaction rate, the experimental data in Figure 9(b and c) were fitted using a numerical reaction kinetics model based on coupled rate equations that take into account the position-dependent attenuation in the PCF due to fibre loss and absorption.[82] Importantly, the model includes only one free parameter: the quantum yield φ of the reaction. Excellent agreement with the experimental data was found for quantum yield values of $\varphi \sim 6.9 \times 10^{-4}$ (at pH 2.5) and $\sim 1.0 \times 10^{-4}$ (at pH 7.5), which are in reasonable agreement with values previously reported in the literature.[173]

3.1.2 Online mass spectrometric determination of photoproducts. The photolysis experiment in the previous section was carried out on a non-flowing liquid sample. Continuous flow measurements in conventional liquid cells (see Figure 2(b)) have a slow response time due to a relatively large dead volume (of the order of 50 μL), which makes it very difficult to analyse irradiated samples online by additional, non-optical methods, even though these might provide more detailed information about transient chemical species. We recently solved this issue by interfacing a HC-PCF with a microfluidic chip (see Figure 2(c)). This allowed the dead volume to be kept to an absolute minimum (sub-μL), resulting in small transition times between consecutive process steps.

As a proof-of-principle experiment, the reaction products of the photoaquation of cyanocobalamin discussed in Section 3.1.1 were flowed directly into an ultrahigh-resolution electrospray-ionisationmass spectrometer (MS) for determination of the reaction products. The results of the analysis are summarised in Figure 10, which shows the mass spectra before (dark) and after irradiation, comparing the reaction performed in a cuvette (Figure 10(a)) with that in the HC-PCF microflow reactor (Figure 10(b)). In both cases the reaction was successful, as evidenced by three new peaks in the mass spectrum that correspond to the photoproduct $[H_2OCbl]^+$ (proved by direct injection of a pure aqueous H_2OCbl solution into the MS, data not shown). We note that cyanocobalamin is still present in both the cuvette and the fibre spectra, though for different reasons. In the cuvette case, the reaction was most probably incomplete. In the fibre case, the total volume flow of analyte through the unilluminated cladding channels is about 6 times higher than through the irradiated fibre core, which introduces unreacted species to the measurement.

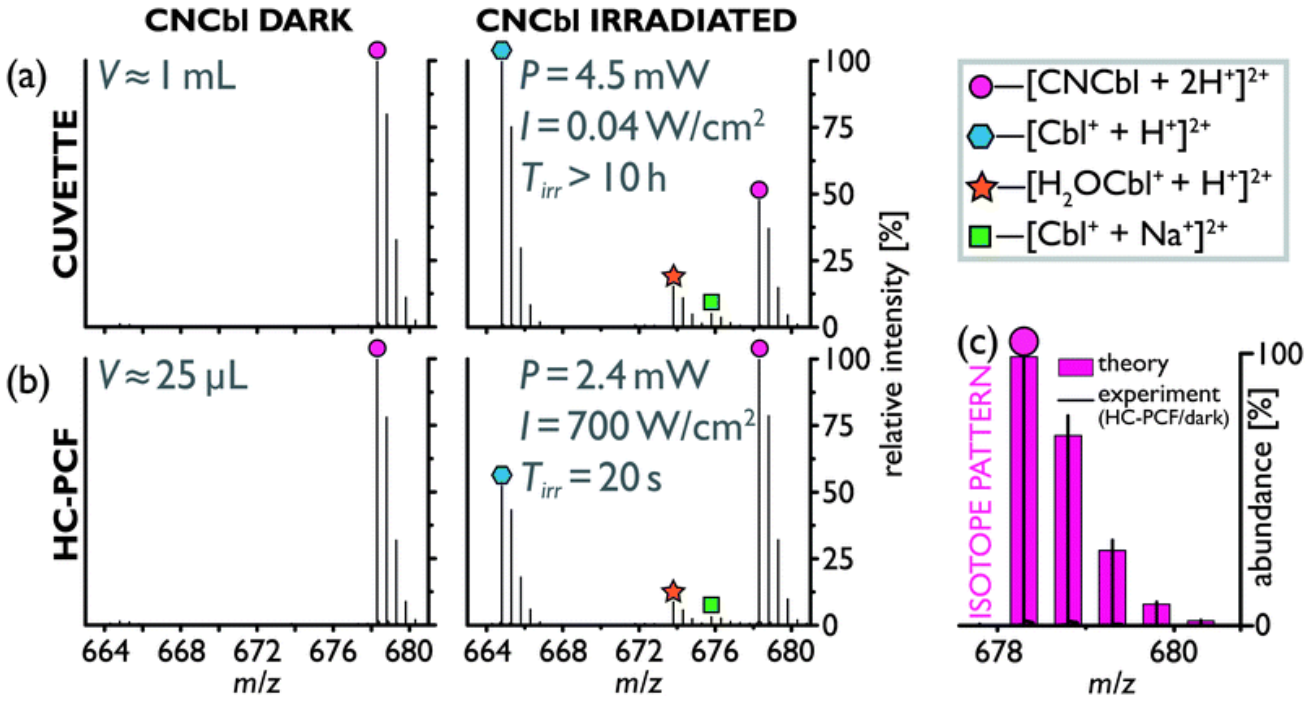

Figure 10. Mass spectra of CNCbl (c = 100 µM) photoaquation (for clarity only the range 663–681 m/z is shown). (a) Conventional approach in a cuvette (irradiated for over 10 hours at 4.5 mW), (b) novel integrated PCF microflow reactor approach (irradiated for 20 s at 2.4 mW; total measurement time: 15 min). The occurrence of ligand-free cobalamin species in the irradiated sample (blue hexagon, green square) is attributed to an artefact resulting from the electrospray ionisation process, in which the weakly-bound water ligand is presumably lost. This was confirmed by the mass spectrum of a directly injected sample of aquacobalamin, not shown. (c) The calculated isotope pattern (pink) matches well the experimental data obtained with the HC-PCF using the ultrahigh-resolution mass spectrometer (black).[84]

The residence time of the chemicals in the fibre core is less than 20 seconds, while the total time required to obtain a maximum signal in the mass spectrometer is 15 min. Hence, the experiment can be performed 50 times faster compared to the conventional approach. Importantly, the sample consumption of this integrated approach is 50 times smaller, resulting in reduced safety risks and improved cost efficiency, which would be particularly important for toxic, scarce or valuable samples.

3.2 Photoisomerisation of azobenzene

Hollow-core PCF has also been used to study the kinetics of thermally reversible photochemical reactions with relatively high quantum yield, such as the photoisomerisation of azobenzene (AB).[175] AB molecules have two stable isomer configurations, *trans* (*E*) and *cis* (*Z*) (see Figure 11(a)), with distinctly different absorption

spectra in the UV-visible wavelength range. The *trans* isomer is the thermally stable species which, under irradiation by a suitable wavelength, is converted to the *cis* isomer. The *cis* isomer can also revert back to the *trans* isomer *via* a photochemical pathway, and normally both isomers absorb light simultaneously until equilibrium between the *trans* and *cis* forms is reached. This state is known as the photostationary state (PSS). After irradiation is switched off, the *cis* isomer thermally relaxes to the *trans* form.[176–179] The compound studied here is a push–pull azobenzene-based dye (ppAB): Disperse Orange 1 (DO1), 4-anilino-4′-nitroazobenzene (see Figure 11(a)). Measuring the quantum yield of ppABs is difficult due to their fast thermal isomerisation rates, which requires that the spectroscopic measurement be near-simultaneous with the photochemical excitation. Furthermore, the high quantum yield requires the use of a low probe intensity to avoid probe-induced photochemistry.[85]

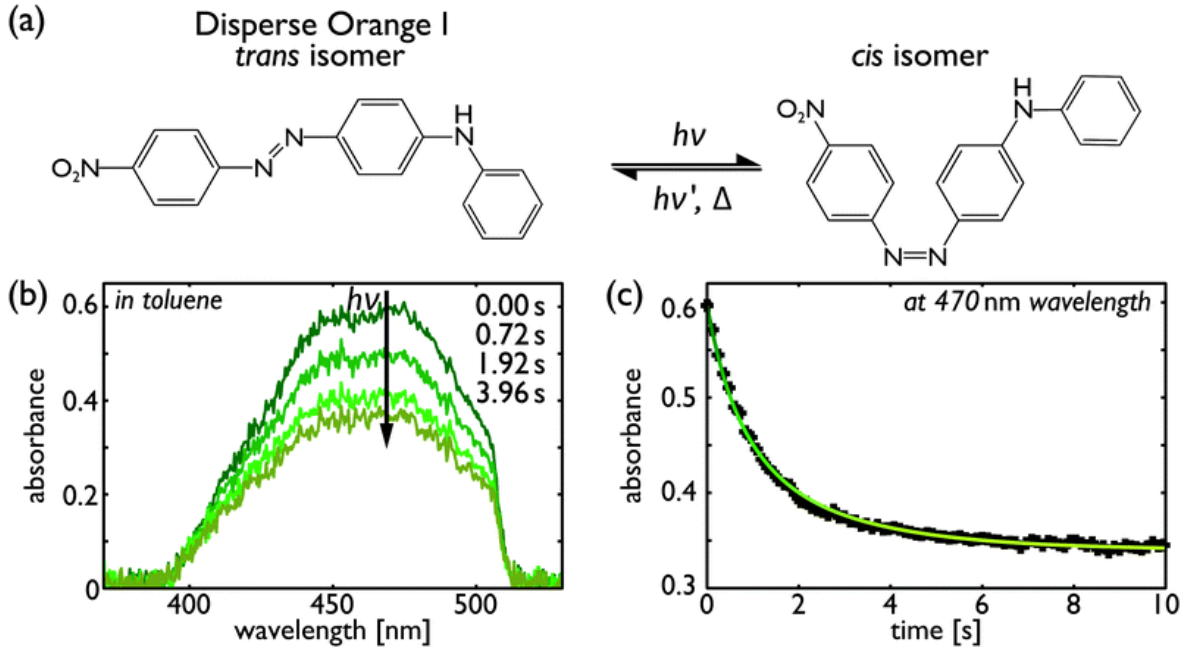

Figure 11. (a) Scheme for the reversible isomerisation of DO1. The forward process occurs only photochemically (*hv*), but the reverse process can proceed photochemically and thermally (Δ). (b)Absorption spectra of 2 μM DO1 in toluene after 0, 0.72 s, 1.92 s and 3.96 s of irradiation. (c) The photoisomerisation kinetics of DO1 in toluene at a concentration of 2 μM, measured at 470 nm, fitted by the theoretical model (curve).[85]

The DO1 sample was pumped into a 30 cm-long kagomé HC-PCF with a core diameter of 19 μm, the total sample volume being only 90 nL. A broadband xenon lamp was used as both photochemical pump and spectroscopic probe. The absorption peak around 450 nm, due to the *trans* isomer, decreases until the PSS is reached in as little as 10 seconds of continuous irradiation, despite the very low excitation power of 0.5 μW

(Figure 11(b)). In a cuvette, almost three orders of magnitude more power was needed to reach the PSS in a comparable time. The measured dynamics of the transition to the PSS were fitted by a kinetics model, in which the total incident intensity of the xenon lamp and spectrally averaged absorption cross-sections were used (Figure 11(c)). This resulted in an estimate of 0.23 for the *trans*-to-*cis* photoisomerisation quantum yield of DO1.[85] To our knowledge this is the first reported measurement of this parameter.

3.3 Catalytic reactions in PCFs

Finally, we discuss the application of PCF as a microreactor for (photo-)catalytic reactions. Two systems are reviewed: the first is based on homogeneous catalysis,[83] in which the catalyst is dispersed in the same phase as the reactants; secondly, we discuss a heterogeneous catalysis system in which catalyst nano-particles are immobilised on the chemically inert glass walls surrounding the core of a HC-PCF.[180,181]

3.3.1 Homogeneous catalysis in PCF (photo-Fenton reaction). As proof-of-principle, a well-known photocatalytic system, the photo-Fenton chemistry[182–185] was studied.[83] A typical application of this reaction is in advanced oxidation processes (AOPs) for water depollution treatment.[186] These processes typically combine UV or visible light irradiation with suitable photo-active catalysts to generate OH radicals, whose high reactivity causes the degradation of organic pollutants such as dyes. For the studies, methylene blue (MB) was used as model dye pollutant, $FeCl_3$ as catalyst, oxalate as ligand, hydrogen peroxide as source for OH radicals, and water as solvent.

The reaction studied here is initiated by excitation of MB with visible light, followed by a reduction of the Fe(III) species by electron transfer from the photo-sensitised dye. Subsequently, hydrogen peroxide is catalytically decomposed by ferrous ions to produce hydroxyl radicals, which in turn, degrade the MB dye (Scheme 2).[183]

$$MB \xrightarrow{h\nu} MB^*$$

$$Fe^{III}(L)_n + MB^* \longrightarrow Fe^{II}(L)_n + MB^{\bullet+}$$

$$Fe^{II}(L)_n + H_2O_2 \longrightarrow Fe^{III}(L)_n + HO^{\bullet} + OH^-$$

$$MB + HO^{\bullet} \longrightarrow \text{degraded products}$$

Scheme 2. Reaction mechanism in the photo-Fenton catalytic process.[183]

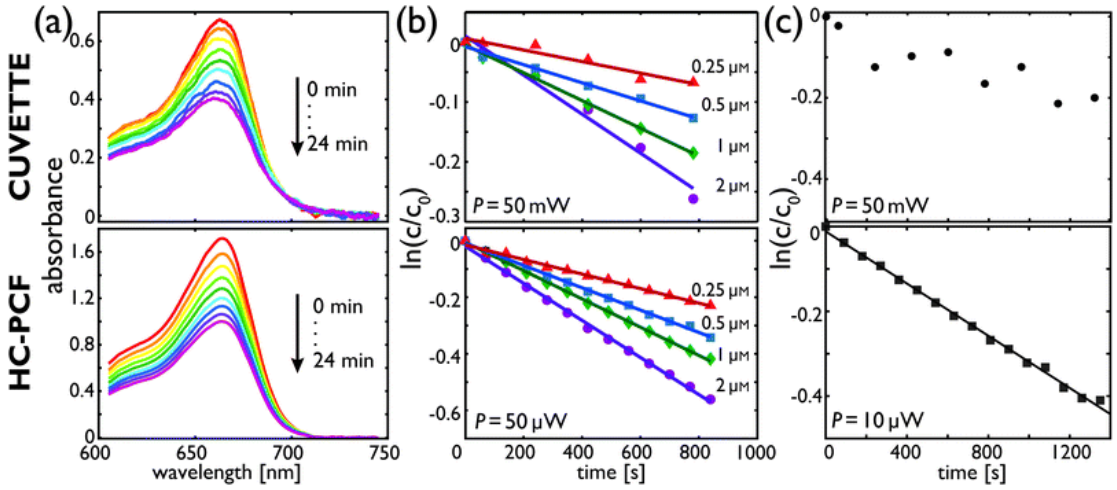

Figure 12. Decolourisation of MB by photo-Fenton chemistry: (a) evolution with time of the absorption spectra of 1 μM MB, 10 μM H_2O_2, 10 μM oxalic acid and 2 μM of $FeCl_3$ in water in a 10 cm cuvette, input power 50 mW (top) and in a 25 cm kagomé HC-PCF, input power 50 μW (bottom). The spectra were taken every 3 min. (b) Temporal relative concentration decay (c, MB concentration and c_0, initial concentration) in the cuvette (top) and in the fibre (bottom) at 664 nm for different catalyst concentrations. (c) Relative concentration decay at 664 nm for a mixture of 0.1 μM MB, 1 μM H_2O_2, 1 μM oxalic acid and 0.2 μM of $FeCl_3$ in the 10 cm cuvette (top) and in a 75 cm kagomé HC-PCF, input power 10 μW (bottom).[83]

The effect of the $FeCl_3$ catalyst concentration on reaction kinetics is summarised in Figure 12(b). As expected, the catalytic activity in both systems increases with catalyst concentration. The activity in the PCF is two times higher than that in the cuvette, which can be attributed to the 100 times higher power density available in the PCF core. Further differences in the kinetics are caused by the variations in emission spectra from the sources used.

To demonstrate the ability of HC-PCF to accurately monitor ultra-low concentration changes, the experiment was repeated with a ten times reduced concentration of all components. Figure 12(c)shows that, at these concentrations, the cuvette measurement (top) becomes very noisy, making accurate measurements impossible. In the HC-PCF, however, whose length was increased to 75 cm to maximise the detection sensitivity, the decolourisation of MB at this ultra-low concentration could be easily monitored, resulting in the smooth decay curve shown in the bottom graph.

3.3.2 Heterogeneous catalysis in PCF (hydrogenation of azobenzene). Finally, we discuss a heterogeneous catalysis system in which catalyst nano-particles are immobilised on the chemically inert glass walls of the HC-PCF. So far, the deposition of metallic nano-particles in PCF has focused on sensing applications such as

surface-enhanced Raman scattering (SERS),[187–191] where optical resonances of Au or Ag nano-particles are employed to strongly enhance the intensity of Raman signals. The homogeneous intensity at the core walls of HC-PCF allows the transmission properties of HC-PCF to be maintained after particle deposition, albeit at increased optical losses.[187–191] Coating techniques include deposition of Ag particles or thin films by high pressure chemical vapour deposition,[187] or by using colloidal solutions of Ag and Au nano-particles.[189] These experiments demonstrate that PCFs can be 'decorated' with nano-particles without significantly impairing light guidance in the fibre. In a similar procedure, we have shown that rhodium (Rh) nano-particles can be deposited by evaporating solvents of precursor liquids that flow through the core of a kagomé HC-PCF.[180] The concentration of the precursor in the solvent influences the final coverage of the fibre with nano-particles and their size distribution. In order to deposit catalyst nano-particles only on the surfaces of the central hollow core of the PCF, the fibre cladding holes were thermally collapsed prior to filling with the precursor.[89] The resulting uniform distribution of Rh nano-particles on the inner fibre surface is shown in Figure 13(a).

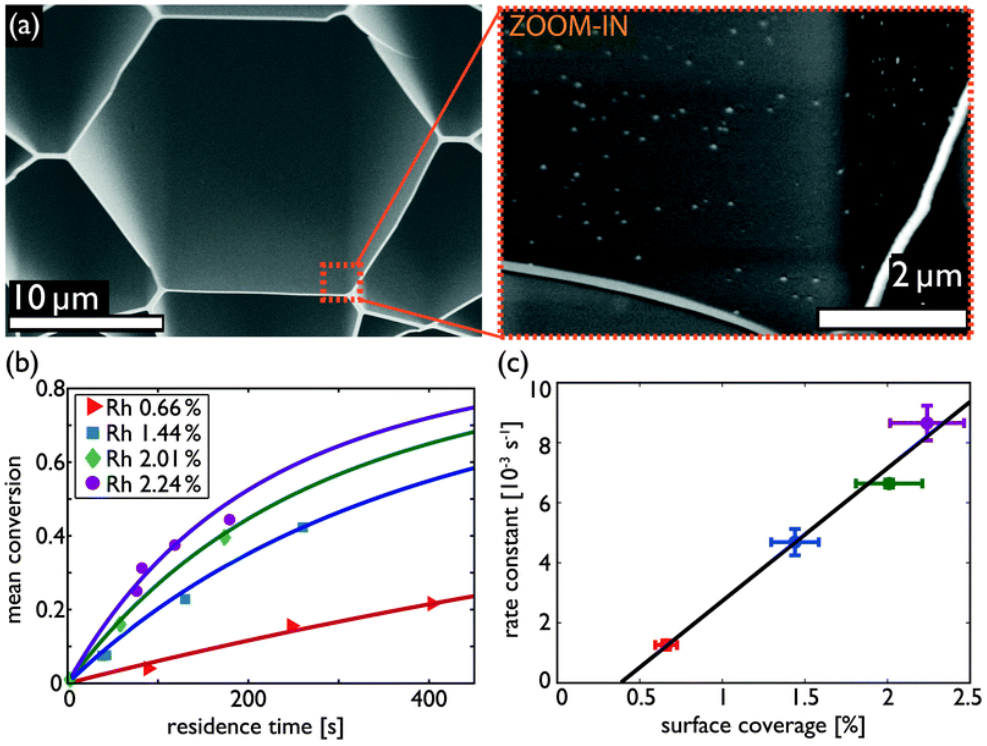

Figure 13. (a) Rh nano-particles deposited in the hollow core of a kagomé HC-PCF, particle size 40 nm. (b) Conversion as a function of the residence time for the hydrogenation of DR1 at 488 nm. (c) Reaction rate constant as a function of the Rh particle surface coverage of the core of the HC-PCF.[181]

The reaction studied in this catalytically active fibre is the well-known catalytic hydrogenation of azobenzene (see Scheme 3).[192] While this particular reaction was not optically driven, it does constitute the first

demonstration of an *in situ* catalytically active HC-PCF microreactor. Liquid-phase experiments were performed on samples of *N*-ethyl-*N*-(2-hydroxyethyl)-4-(4-nitrophenylazo)aniline (commercially known as Disperse Red 1, DR1), dissolved in isopropanol and at room temperature. The substrate passes through a hydrogen gas saturator prior to being pumped through the fibre. The hydrogen pressure is also used to adjust the flow rate and, with that, the residence time of the reactants inside the continuous-flow HC-PCF reactor. The hydrogenation of DR1 causes a shift of the main absorption peak towards shorter wavelengths in the UV,[193] which was monitored online by in-fibre absorption spectroscopy.

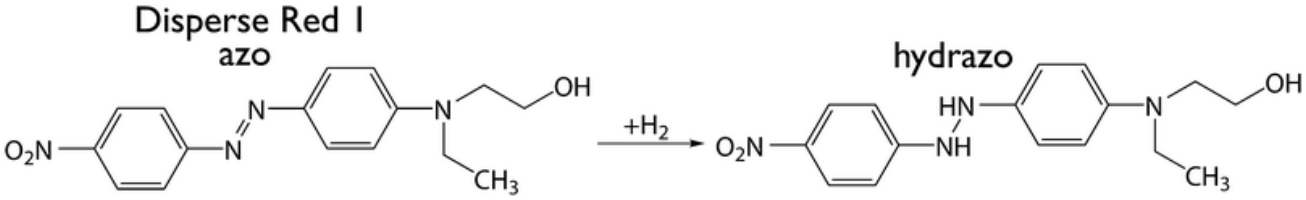

Scheme 3. Reaction mechanism for the hydrogenation of the azobenzene-based dye DR1.[192]

The conversion rate of a 1 μM DR1 sample was studied by monitoring the transmission at 488 nm in four HC-PCFs with Rh particle surface coverage ranging from 0.66 to 2.24%. The hydrogen pressure was varied from 1 to 10 bar, causing the residence time to increase from 40 to 400 s (data points in Figure 13(b)). The experimental results obtained for the catalytic fibre reactor were modelled using the classical reaction engineering solution for plug-flow tubular reactors (PFTR).[194] The measured data agreed well with a modified first order reaction kinetics model, which takes into account the DR1 concentration gradient along the HC-PCF (solid lines, Figure 13(b)). The reaction rate constant, the single free parameter in the model, was obtained for the four fibres, each being prepared with a different catalyst precursor concentration. By comparing the rate constants with the particle surface coverage obtained from SEM images, we found a linear dependence between these two parameters (Figure 13(c)).

Although these results are for liquid-phase heterogeneous catalysis, the procedure could also be transferred to gas-phase catalysis. A proof-of-concept experiment using hollow capillaries was given,*e.g.*, for the hydrogenation of ethylene to ethane.[180]

4. Conclusions and outlook

The chemical processes reported in this review paper demonstrate that photonic crystal fibres can be used as versatile sensors and highly efficient microreactors for a wide range of photochemical and catalytic reactions. Several important advantages of PCF over conventional systems were discussed:

(1) The narrow optofluidic channels in the PCF reduce the sample volume by up to six orders of magnitude compared to conventional cuvettes (Chapter 1).

(2) Low transmission losses permit path-lengths of up to several metres, allowing measurements at extremely low analyte concentrations (Chapter 2).

(3) The tight confinement of light and sample in the fibre core results in strongly enhanced light-matter interactions, allowing measurements of low quantum yield photochemical reactions (Chapter 3.1).

(4) The reaction kinetics can be conveniently monitored by *in situ* spectroscopic methods (Chapter 3).

(5) In continuous-flow arrangements, non-optical analytical methods such as mass spectrometry can be used (Chapter 3.1).

(6) The inner surface of the PCF can be made chemically active by surface modification methods (Chapter 3.3).

It is clear that the examples described in this paper represent only a small sample from a huge number of photochemical reactions that can potentially profit from being investigated in a PCF. For instance, a field that could greatly benefit from the use of PCF microreactors is that of photoactive anti-cancer compounds, where reaction schemes depend critically on the irradiation conditions. It might be possible to initiate specific photochemical reactions selectively, *e.g.*, by choice of the wavelength. This could be useful in the development of excited-state drugs, in which selective excitation of particular electronic transitions of metal complexes leads to control of the decomposition pathways.[162] Furthermore, high intensities in the fibre core would allow the use of two-photon excitation mechanisms. Photo-assisted chemical synthesis[164,195–197] for industrial processes can also benefit from the controlled and high irradiance provided by optofluidic PCFs used as microflow reactors.

On the technical side, the development of a robust, easy-to-use, all-fibre optofluidic photoreactor can be envisaged, in which fibre lasers or PCF-based supercontinuum sources could be integrated with the sample-containing PCF. The incorporation of PCFs as photochemical reactors in lab-on-a-chip devices[143–145] could revolutionise high-throughput screening of photoactive targets. The output of such a device could be coupled to additional analytical techniques such as mass spectrometry, nuclear magnetic resonance spectroscopy or electron paramagnetic resonance spectroscopy. Such coupled methods could be helpful for the detection of short-lived reaction species, which are undetectable using conventional techniques.

Furthermore, surface-modified PCFs decorated with catalyst nano-particles may allow monitoring the catalytic species, which could raise new possibilities for a combined mechanistic and kinetic understanding.

Apart from chemistry, other areas such as biomedicine could also benefit from the outstanding properties of PCF. In therapy, for example, high intensity light needs to be delivered rapidly and accurately to local areas of the body if tumours are to be destroyed selectively with little damage to surrounding normal tissues. The microfluidic channels of PCF could be used to both deliver light and the photodrug to the specific sites needed. They can also be used in chromatography,[198–201] a multiplicity of identical narrow channels providing good discrimination between different compounds.

Notes and references

[†]The expression assumes zero dispersion.

[‡]Since the rotation is connected to the quantum yield, lifetime and emission, rhodamine B is typically used as a fluorescent temperature probe, see *e.g.* M. A. Bennet, P. R. Richardson, J. Arlt, A. McCarthy, G. S. Buller and A. C. Jones, *Lab. Chip*, 2011, **11**, 3821–3828.

[1] J. M. López-Higuera, *Handbook of optical fibre sensing technology*, John Wiley & Sons Ltd., Chichester, England, 1st edn, 2002.

[2] O. S. Wolfbeis, *Anal. Chem.*, 2004, **76**, 3269–3284.

[3] G. Stewart, W. Jin and B. Culshaw, *Sens. Actuators, B*, 1997, **38**, 42–47.

[4] A. Leung, P. M. Shankar and R. Mutharasan, *Sens. Actuators, B*, 2007, **125**, 688–703.

[5] A. P. Abel, M. G. Weller, G. L. Duveneck, M. Ehrat and H. M. Widmer, *Anal. Chem.*, 1996, **68**, 2905–2912.

[6] J. I. Peterson and G. G. Vurek, *Science*, 1984, **224**, 123–127.

[7] B. I. Bluestein, I. M. Walczak and S.-Y. Chen, *Trends Biotechnol.*, 1990, **8**, 161–168.

[8] K. R. Rogers and E. J. Poziomek, *Chemosphere*, 1996, **33**, 1151–1174.

[9] G. Whitenett, G. Stewart, K. Atherton, B. Culshaw and W. Johnstone, *J. Opt. A: Pure Appl. Opt.*, 2003, **5**, S140–S145.

[10] A. A. Veselov, B. G. Abraham, H. Lemmetyinen, M. T. Karp and N. V. Tkachenko, *Anal. Bioanal. Chem.*, 2012, 1–10.

[11] S.-M. Tseng and C.-L. Chen, *Appl. Opt.*, 1992, **31**, 3438–3447.

[12] S. M. Chandani and N. A. Jaeger, *IEEE Photon. Technol. Lett.*, 2005, **17**, 2706–2708.

[13] J. Villatoro, A. Díez, J. L. Cruz and M. V. Andres, *IEEE Sens. J.*, 2003, **3**, 533–537.

[14] B. D. Gupta, H. Dodeja and A. K. Tomar, *Opt. Quantum Electron.*, 1996, **28**, 1629–1639.

[15] H. Schmidt and A. R. Hawkins, *Microfluid. Nanofluid.*, 2008, **4**, 3–16.

[16] L. J. Gimbert and P. J. Worsfold, *TrAC, Trends Anal. Chem.*, 2007, **26**, 914–930.

[17] M. E. Lippitsch, S. Draxler, D. Kieslinger, H. Lehmann and B. H. Weigl, *Appl. Opt.*, 1996, **35**, 3426–3431.

[18] Y. Fink, D. J. Ripin, S. Fan, C. Chen, J. D. Joannopoulos and E. L. Thomas, *J. Lightwave Technol.*, 1999, **17**, 2039–2041.

[19] H. Qu and M. Skorobogatiy, *Appl. Phys. Lett.*, 2011, **98**, 201114.

[20] A. M. Stolyarov, A. Gumennik, W. McDaniel, O. Shapira, B. Schell, F. Sorin, K. Kuriki, G. Benoit, A. Rose, J. D. Joannopoulos and Y. Fink, *Opt. Express*, 2012, **20**, 12407–12415.

[21] D. Yin, H. Schmidt, J. P. Barber, E. J. Lunt and A. R. Hawkins, *Opt. Express*, 2005, **13**, 10564–10570.

[22] D. Yin, D. W. Deamer, H. Schmidt, J. P. Barber and A. R. Hawkins, *Appl. Phys. Lett.*, 2004, **85**, 3477–3479.

[23] H. Schmidt and A. R. Hawkins, *Nat. Photonics*, 2011, **5**, 598–604.

[24] K. J. Rowland, S. Afshar, A. Stolyarov, Y. Fink and T. M. Monro, *Opt. Express*, 2012, **20**, 48–62.

[25] P. St. J. Russell, *Science*, 2003, **299**, 358–362.

[26] P. St. J. Russell, *J. Lightwave Technol.*, 2006, **24**, 4729–4749.

[27] E. Yablonovitch, *Phys. Rev. Lett.*, 1987, **58**, 2059–2062.

[28] S. John, *Phys. Rev. Lett.*, 1987, **58**, 2486–2489.

[29] P. St. J. Russell, *Opt. Photonics News*, 2007, **18**, 26–31.

[30] R. F. Cregan, B. J. Mangan, J. C. Knight, T. A. Birks, P. St. J. Russell, P. J. Roberts and D. C. Allan, *Science*, 1999, **285**, 1537–1539.

[31] P. J. Roberts, F. Couny, H. Sabert, B. J. Mangan, D. P. Williams, L. Farr, M. W. Mason, A. Tomlinson, T. A. Birks, J. C. Knight and P. St. J. Russell, *Opt. Express*, 2005, **13**, 236–244.

[32] T. A. Birks, J. C. Knight and P. St. J. Russell, *Opt. Lett.*, 1997, **22**, 961–963.

[33] X. Fan and I. M. White, *Nat. Photonics*, 2011, **5**, 591–597.

[34] A. R. Hawkins and H. Schmidt, *Handbook of optofluidics*, CRC Press Inc., 1st edn, 2010.

[35] C. Monat, P. Domachuk and B. J. Eggleton, *Nat. Photonics*, 2007, **1**, 106–114.

[36] J. C. Knight, T. A. Birks, P. St. J. Russell and D. M. Atkin, *Opt. Lett.*, 1996, **21**, 1547–1549.

[37] J. C. Knight, T. A. Birks, R. F. Cregan, P. St. J. Russell and J. P. de Sandro, *Electron. Lett.*, 1998, **34**, 1347–1348.

[38] A. Ortigosa-Blanch, J. C. Knight, W. J. Wadsworth, J. Arriaga, B. J. Mangan, T. A. Birks and P. St. J. Russell, *Opt. Lett.*, 2000, **25**, 1325–1327.

[39] N. G. R. Broderick, T. M. Monro, P. J. Bennett and D. J. Richardson, *Opt. Lett.*, 1999, **24**, 1395–1397.

[40] J. C. Knight, J. Arriaga, T. A. Birks, A. Ortigosa-Blanch, W. J. Wadsworth and P. St. J. Russell, *IEEE Photon. Technol. Lett.*, 2000, **12**, 807–809.

[41] K. Kurokawa, K. Nakajima, K. Tsujikawa, T. Yamamoto and K. Tajima, *J. Lightwave Technol.*, 2009, **27**, 1653–1662.

[42] J. M. Dudley, G. Genty and S. Coen, *Rev. Mod. Phys.*, 2006, **78**, 1135–1184.

[43] C. F. Kaminski, R. S. Watt, A. D. Elder, J. H. Frank and J. Hult, *Appl. Phys. B: Lasers Opt.*, 2008, **92**, 367–378.

[44] J. M. Langridge, T. Laurila, R. S. Watt, R. L. Jones, C. F. Kaminski and J. Hult, *Opt. Express*, 2008, **16**, 10178–10188.

[45] D. K. Wu, B. T. Kuhlmey and B. J. Eggleton, *Opt. Lett.*, 2009, **34**, 322–324.

[46] W. J. Wadsworth, A. Ortigosa-Blanch, J. C. Knight, T. A. Birks, T. P. M. Man and P. St. J. Russell, *J. Opt. Soc. Am. B*, 2002, **19**, 2148–2155.

[47] G. Humbert, W. J. Wadsworth, S. G. Leon-Saval, J. C. Knight, T. A. Birks, P. St. J. Russell, M. J. Lederer, D. Kopf, K. Wiesauer, E. I. Breuer and D. Stifter, *Opt. Express*, 2006, **14**, 1596–1603.

[48] A. Aguirre, N. Nishizawa, J. Fujimoto, W. Seitz, M. Lederer and D. Kopf, *Opt. Express*, 2006, **14**, 1145–1160.

[49] J. M. Fini, *Meas. Sci. Technol.*, 2004, **15**, 1120–1128.

[50] T. M. Monro, W. Belardi, K. Furusawa, J. C. Baggett, N. Broderick and D. J. Richardson, *Meas. Sci. Technol.*, 2001, **12**, 854–858.

[51] M. T. Myaing, J. Y. Ye, T. B. Norris, T. Thomas, J. R. Baker Jr., W. J. Wadsworth, G. Bouwmans, J. C. Knight and P. St. J. Russell, *Opt. Lett.*, 2003, **28**, 1224–1226.

[52] J. B. Jensen, P. E. Hoiby, G. Emiliyanov, O. Bang, L. H. Pedersen and A. Bjarklev, *Opt. Express*, 2005, **13**, 5883–5889.

[53] Y. L. Hoo, W. Jin, H. L. Ho, D. N. Wang and R. S. Windeler, *Opt. Eng.*, 2002, **41**, 8–9.

[54] C. M. B. Cordeiro, M. A. R. Franco, G. Chesini, E. C. S. Barretto, R. Lwin, C. H. Brito Cruz and M. C. J. Large, *Opt. Express*, 2006, **14**, 13056–13066.

[55] L. Rindorf, J. B. Jensen, M. Dufva, L. H. Pedersen, P. E. Høiby and O. Bang, *Opt. Express*, 2006, **14**, 8224–8231.

[56] C. M. B. Cordeiro, C. J. S. de Matos, E. M. dos Santos, A. Bozolan, J. S. K. Ong, T. Facincani, G. Chesini, A. R. Vaz and C. H. Brito Cruz, *Meas. Sci. Technol.*, 2007, **18**, 3075–3081.

[57] C. M. B. Cordeiro, E. M. dos Santos, C. H. Brito Cruz, C. J. S. de Matos and D. S. Ferreira, *Opt. Express*, 2006, **14**, 8403–8412.

[58] F. M. Cox, R. Lwin, M. C. J. Large and C. M. B. Cordeiro, *Opt. Express*, 2007, **15**, 11843–11848.

[59] C. Martelli, P. Olivero, J. Canning, N. Groothoff, B. Gibson and S. Huntington, *Opt. Lett.*, 2007, **32**, 1575–1577.

[60] A. van Brakel, C. Grivas, M. N. Petrovich and D. J. Richardson, *Opt. Express*, 2007, **15**, 8731–8736.

[61] C. Hensley, D. H. Broaddus, C. B. Schaffer and A. L. Gaeta, *Opt. Express*, 2007, **15**, 6690–6695.

[62] T. M. Monro, D. J. Richardson and P. J. Bennett, *Electron. Lett.*, 1999, **35**, 1188–1189.

[63] A. S. Webb, F. Poletti, D. J. Richardson and J. K. Sahu, *Opt. Eng.*, 2007, **46**, 010503.

[64] T. M. Monro, S. Warren-Smith, E. P. Schartner, A. François, S. Heng, H. Ebendorff-Heidepriem and S. Afshar, *Opt. Fiber Technol.*, 2010, **16**, 343–356.

[65] T. G. Euser, J. S. Y. Chen, M. Scharrer, P. St. J. Russell, N. J. Farrer and P. J. Sadler, *J. Appl. Phys.*, 2009, **103**, 103108.

[66] G. O. S. Williams, T. G. Euser, P. St. J. Russell and A. C. Jones, *Methods Appl. Fluoresc.*, 2013, **1**, 015003.

[67] F. Benabid, *Philos. Trans. R. Soc., A*, 2006, **364**, 3439–3462.

[68] M. H. Frosz, J. Nold, T. Weiss, A. Stefani, S. Rammler, F. Babic and P. St. J. Russell, *Frontiers in Optics*, Rochester, NY, 2012.

[69] B. J. Mangan, L. Farr, A. Langford, P. J. Roberts, D. P. Williams, F. Couny, M. Lawman, M. Mason, S. Coupland, R. Flea, H. Sabert, T. A. Birks, J. C. Knight and P. St. J. Russell, Optical Fiber Communication Conference (OFC 2004), Los Angeles, California, 2004.

[70] G. J. Pearce, J. M. Pottage, D. M. Bird, P. J. Roberts, J. C. Knight and P. St. J. Russell, *Opt. Express*, 2005, **13**, 6937–6946.

[71] J. D. Shephard, W. N. MacPherson, R. R. J. Maier, J. D. C. Jones, D. P. Hand, M. Mohebbi, A. K. George, P. J. Roberts and J. C. Knight, *Opt. Express*, 2005, **13**, 7139–7144.

[72] T. Ritari, J. Tuominen, H. Ludvigsen, J. C. Petersen, T. Sørensen, T. P. Hansen and H. R. Simonsen, *Opt. Express*, 2004, **12**, 4080–4087 .

[73] A. M. Cubillas, M. Silva-Lopez, J. M. Lazaro, O. M. Conde, M. N. Petrovich and J. M. Lopez-Higuera, *Opt. Express*, 2007, **15**, 17570–17576.

[74] L. W. Kornaszewski, N. Gayraud, J. M. Stone, W. N. MacPherson, A. K. George, J. C. Knight, D. P. Hand and D. T. Reid, *Opt. Express*, 2007, **15**, 11219–11224.

[75] A. M. R. Pinto and M. Lopez-Amo, *J. Sens.*, 2012, **2012**, 598178.

[76] F. Benabid, F. Couny, J. C. Knight, T. A. Birks and P. St. J. Russell, *Nature*, 2005, **434**, 488–491.

[77] F. Benabid, J. C. Knight, G. Antonopoulos and P. St. J. Russell, *Science*, 2002, **298**, 399–402.

[78] F. Couny, F. Benabid and P. S. Light, *Opt. Lett.*, 2006, **31**, 3574–3576.

[79] G. J. Pearce, G. S. Wiederhecker, C. G. Poulton, S. Burger and P. St. J. Russell, *Opt. Express*, 2007, **15**, 12680–12685.

[80] Y. Y. Wang, X. Peng, M. Alharbi, C. F. Dutin, T. D. Bradley, F. Gérôme, M. Mielke, T. Booth and F. Benabid, *Opt. Lett.*, 2012, **37**, 3111–3113.

[81] F. Yu, W. J. Wadsworth and J. C. Knight, *Opt. Express*, 2012, **20**, 11153–11158.

[82] J. S. Y. Chen, T. G. Euser, N. J. Farrer, P. J. Sadler, M. Scharrer and P. St. J. Russell, *Chem.–Eur. J.*, 2010, **16**, 5607–5612.

[83] A. M. Cubillas, M. Schmidt, M. Scharrer, T. G. Euser, B. J. M. Etzold, N. Taccardi, P. Wasserscheid and P. St. J. Russell, *Chem.–Eur. J.*, 2012, **18**, 1586–1590.

[84] S. Unterkofler, R. J. McQuitty, T. G. Euser, N. J. Farrer, P. J. Sadler and P. St. J. Russell, *Opt. Lett.*, 2012, **37**, 1952–1954.

[85] G. O. S. Williams, J. S. Y. Chen, T. G. Euser, P. St. J. Russell and A. C. Jones, *Lab Chip*, 2012, **12**, 3356–3361.

[86] S. Yiou, P. Delaye, A. Rouvie, J. Chinaud, R. Frey, G. Roosen, P. Viale, S. Février, P. Roy and J.-L. Auguste, *Opt. Express*, 2005, **13**, 4786–4791.

[87] K. Nielsen, D. Noordegraaf, T. Sørensen, A. Bjarklev and T. P. Hansen, *J. Opt. A: Pure Appl. Opt.*, 2005, **7**, L13–L20.

[88] Y. Huang, Y. Xu and A. Yariv, *Appl. Phys. Lett.*, 2004, **85**, 5182–5184.

[89] L. Xiao, W. Jin, M. S. Demokan, H. L. Ho, Y. L. Hoo and C.-l. Zhao, *Opt. Express*, 2005, **13**, 9014–9022.

[90] T. A. Birks, D. M. Bird, T. D. Hedley, J. M. Pottage and P. St. J. Russell, *Opt. Express*, 2004, **12**, 69–74.

[91] G. Antonopoulos, F. Benabid, T. A. Birks, D. M. Bird, J. C. Knight and P. St. J. Russell, *Opt. Express*, 2006, **14**, 3000–3006.

[92] F. M. Cox, A. Argyros and M. C. J. Large, *Opt. Express*, 2006, **14**, 4135–4140.

[93] A. C. Tam and C. K. N. Patel, *Appl. Opt.*, 1979, **18**, 3348–3358.

[94] S. Ghosh, A. R. Bhagwat, C. K. Renshaw, S. Goh, A. L. Gaeta and B. J. Kirby, *Phys. Rev. Lett.*, 2006, **97**, 023603.

[95] L. Xiao, T. A. Birks and W. Loh, *Opt. Lett.*, 2011, **36**, 4662–4664.

[96] E. A. J. Marcatili and R. A. Schmeltzer, *Bell Syst. Tech. J.*, 1964, **43**, 1783–1809.

[97] T. P. Hansen, J. Broeng, C. Jakobsen, G. Vienne, H. R. Simonsen, M. D. Nielsen, P. M. Skovgaard, J. R. Folkenberg and A. Bjarklev, *J. Lightwave Technol.*, 2004, **22**, 11.

[98] A. Bhardwaj, B. Beaudou, F. Gérôme, G. Humbert, J.-L. Auguste, J.-M. Blondy and F. Benabid, 37th European Conference and Exhibition on Optical Communication (ECOC 2011), Geneva, Switzerland, 2011.

[99] J. Hodgkinson and R. P. Tatam, *Meas. Sci. Technol.*, 2013, **24**, 012004.

[100] F. K. Tittel, *Appl. Phys. B: Lasers Opt.*, 1998, **67**, 339–345.

[101] G. Stewart, B. Culshaw, W. Johnstone, G. Whitenett, K. Atherton and A. McLean, *Manag. Environ. Qual. Int. J.*, 2003, **14**, 181–190.

[102] G. Wysocki, A. A. Kosterev and F. K. Tittel, *Appl. Phys. B: Lasers Opt.*, 2005, **80**, 617–625.

[103] M. B. Pushkarsky, M. E. Webber, O. Baghdassarian, L. R. Narasimhan and C. K. N. Patel, *Appl. Phys. B: Lasers Opt.*, 2002, **75**, 391–396.

[104] B. Culshaw, W. Johnstone, G. Stewart, K. Duffin, I. S. Mauchline, D. Walsh, 9th IMVC Mine Ventilation Conference, Delhi, India, 2009.

[105] U. Willer, M. Saraji, A. Khorsandi, P. Geiser and W. Schade, *Opt. Laser Eng.*, 2006, **44**, 699–710.

[106] M. Mürtz, D. Halmer, M. Horstjann, S. Thelen and P. Hering, *Spectrochim. Acta, Part A*, 2006, **63**, 963–969.

[107] P. Mirtaheri, T. Omtveit, T. Klotzbuecher, S. Grimnes, Ø. G. Martinsen and T. I. Tønnessen, *Physiol. Meas.*, 2004, **25**, 1511–1522.

[108] P. Werle, F. Slemr, K. Maurer, R. Kormann, R. Mücke and B. Jänker, *Opt. Laser Eng.*, 2002, **37**, 101–114.

[109] D. R. Herriott and H. J. Schulte, *Appl. Opt.*, 1965, **4**, 883–889.

[110] J. B. McManus, P. L. Kebabian and M. Zahniser, *Appl. Opt.*, 1995, **34**, 3336–3348.

[111] J. U. White, *J. Opt. Soc. Am.*, 1942, **32**, 285–288.

[112] S.-G. Li, S.-Y. Liu, Z.-Y. Song, Y. Han, T.-L. Cheng, G.-Y. Zhou and L.-T. Hou, *Appl. Opt.*, 2007, **46**, 5183–5188.

[113] J. Chen, A. Hangauer, R. Strzoda, T. G. Euser, J. S. Y. Chen, M. Scharrer, P. St. J. Russell and M.-C. Amann, Conference on Lasers and Electro-Optics (CLEO 2010), San Jose, California, USA, 2010.

[114] G. Yan, A. P. Zhang, G. Ma, B. Wang, B. Kim, J. Im, S. He and Y. Chung, *IEEE Photon. Technol. Lett.*, 2011, **23**, 1588–1590.

[115] V. Matejec, J. Mrázek, M. Hayer, I. Kašík, P. Peterka, J. Kaňka, P. Honzátko and D. Berková, *Mater. Sci. Eng., C*, 2006, **26**, 317–321.

[116] Y. L. Hoo, W. Jin, H. L. Ho, J. Ju and D. N. Wang, *Sens. Actuators, B*, 2005, **105**, 183–186.

[117] J. Pawłat, T. Sugiyama, T. Matsuo and T. Ueda, *Plasma Processes Polym.*, 2007, **4**, 743–752.

[118] A. M. Cubillas, J. M. Lazaro, M. Silva-Lopez, O. M. Conde, M. N. Petrovich and J. M. Lopez-Higuera, *Electron. Lett.*, 2008, **44**, 403–404.

[119] N. Gayraud, Ł. W. Kornaszewski, J. M. Stone, J. C. Knight, D. T. Reid, D. P. Hand and W. N. MacPherson, *Appl. Opt.*, 2008, **47**, 1269–1277.

[120] H. Lehmann, H. Bartelt, R. Willsch, R. Amezcua-Correa and J. C. Knight, *IEEE Sens. J.*, 2011, **11**, 2926–2931.

[121] X. Li, J. Liang, S. Lin, Y. Zimin, Y. Zhang and T. Ueda, *IEEE Sens. J.*, 2012, **12**, 2362–2367.

[122] J. A. Nwaboh, J. Hald, J. K. Lyngsø, J. C. Petersen and O. Werhahn, *Appl. Phys. B: Lasers Opt.*, 2012, 1–8.

[123] J. P. Carvalho, H. Lehmann and H. Bartelt, *et al.*, *J. Sens.*, 2009, **2009**, 398403.

[124] A. M. Cubillas, J. Hald and J. C. Petersen, *Opt. Express*, 2008, **16**, 3976–3985.

[125] E. Austin, A. van Brakel, M. N. Petrovich and D. J. Richardson, *Sens. Actuators, B*, 2009, **139**, 30–34.

[126] A. van Brakel, C. Jáuregui Misas, T. T. Ng, P. Petropoulos, J. P. Dakin, C. Grivas, M. N. Petrovich and D. J. Richardson, Conference on Lasers and Electro-Optics (CLEO 2008), San Jose, California, USA, 2008.

[127] A. M. Cubillas, J. M. Lazaro, O. M. Conde, M. N. Petrovich and J. M. Lopez-Higuera, *Sensors*, 2009, **9**, 490–502.

[128] R. M. Mihalcea, D. S. Baer and R. K. Hanson, *Appl. Opt.*, 1997, **36**, 8745–8752.

[129] J. Henningsen and J. Hald, *Appl. Opt.*, 2008, **47**, 2790–2797.

[130] R. M. Wynne, B. Barabadi, K. J. Creedon and A. Ortega, *J. Lightwave Technol.*, 2009, **27**, 1590–1596.

[131] Y. L. Hoo, W. Jin, C. Shi, H. L. Ho, D. N. Wang and S. C. Ruan, *Appl. Opt.*, 2003, **42**, 3509–3515.

[132] Y. L. Hoo, S. Liu, H. L. Ho and W. Jin, *IEEE Photon. Technol. Lett.*, 2010, **22**, 296–298.

[133] J. P. Parry, B. C. Griffiths, N. Gayraud, E. D. McNaghten, A. M. Parkes, W. N. MacPherson and D. P. Hand, *Meas. Sci. Technol.*, 2009, **20**, 075301.

[134] J. Henningsen, J. Hald and J. C. Petersen, *Opt. Express*, 2005, **13**, 10475–10482.

[135] R. Thapa, K. Knabe, M. Faheem, A. Naweed, O. L. Weaver and K. L. Corwin, *Opt. Lett.*, 2006, **31**, 2489–2491.

[136] J. Tuominen, T. Ritari, H. Ludvigsen and J. C. Petersen, *Opt. Commun.*, 2005, **255**, 272–277.

[137] F. Benabid, P. S. Light, F. Couny and P. St. J. Russell, *Opt. Express*, 2005, **13**, 5694–5703.

[138] A. R. Bhagwat and A. L. Gaeta, *Opt. Express*, 2008, **16**, 5035–5047.

[139] J. C. Travers, W. Chang, J. Nold, N. Y. Joly and P. St. J. Russell, *J. Opt. Soc. Am. B*, 2011, **28**, A11–A26.

[140] H. C. Hunt and J. S. Wilkinson, *Microfluid. Nanofluid.*, 2008, **4**, 53–79.

[141] L. Pang, H. Matthew Chen, L. M. Freeman and Y. Fainman, *Lab Chip*, 2012, **12**, 3543–3551.

[142] Y. Fainman, L. Lee, D. Psaltis and C. Yang, *Optofluidics: fundamentals, devices, and applications*, McGraw-Hill Professional, New York, USA, 1st edn, 2010.

[143] T. M. Squires and S. R. Quake, *Rev. Mod. Phys.*, 2005, **77**, 977–1026.

[144] A. J. Demello, *Nature*, 2006, **442**, 394–402.

[145] G. M. Whitesides, *Nature*, 2006, **442**, 368–373.

[146] C. Pollock and M. Lipson, *Integrated photonics*, Kluwer Academic Publishers, Massachusetts, USA, 1st edn, 2003.

[147] G. Lifante, *Integrated photonics: fundamentals*, John Wiley & Sons Ltd., Chichester, England, 1st edn, 2003.

[148] R. G. Hunsberger, *Integrated Optics: Theory and Technology*, Springer, New York, USA, 6th edn, 2009.

[149] W. Lukosz, *Biosens. Bioelectron.*, 1991, **6**, 215–225.

[150] W. Henry, *Opt. Quantum Electron.*, 1994, **26**, 261–272.

[151] J. B. Jensen, L. H. Pedersen, P. E. Hoiby, L. B. Nielsen, T. P. Hansen, J. R. Folkenberg, J. Riishede, D. Noordegraaf, K. Nielsen, A. Carlsen and A. Bjarklev, *Opt. Lett.*, 2004, **29**, 1974–1976.

[152] J. R. Lakowicz, *Principles of fluorescence spectroscopy*, Springer, New York, USA, 3rd edn, 2006.

[153] S. O. Konorov, A. M. Zheltikov and M. Scalora, *Opt. Express*, 2005, **13**, 3454–3459.

[154] Y. Ruan, E. P. Schartner, H. Ebendorff-Heidepriem, P. Hoffmann and T. M. Monro, *Opt. Express*, 2007, **15**, 17819–17826.

[155] S. Afshar V, S. C. Warren-Smith and T. M. Monro, *Opt. Express*, 2007, **15**, 17891–17901.

[156] S. Smolka, M. Barth and O. Benson, *Opt. Express*, 2007, **151**, 12783.

[157] F. López Arbeloa, T. López Arbeloa, M. J. Tapia Estevez and I. López Arbeloa, *J. Phys. Chem.*, 1991, **95**, 2203–2208.

[158] T. A. Smith, M. Irwanto, D. J. Haines, K. P. Ghiggino and D. P. Millar, *Colloid Polym. Sci.*, 1998, **276**, 1032–1037 .

[159] K. G. Casey and E. L. Quitevis, *J. Phys. Chem.*, 1988, **92**, 6590–6594 .

[160] N. J. Turro, V. Ramamurthy and J. C. Scaiano, *Principles of molecular photochemistry: an introduction*, University Science Books, USA, 1st edn, 2009.

[161] C. Robertson, D. H. Evans and H. Abrahamse, *J. Photochem. Photobiol., B*, 2009, **96**, 1–8.

[162] N. J. Farrer, L. Salassa and P. J. Sadler, *Dalton Trans.*, 2009, 10690–10701.

[163] D. Phillips, *Pure Appl. Chem.*, 1995, **67**, 117–126.

[164] N. Hoffmann, *Chem. Rev.*, 2008, **108**, 1052.

[165] H. Spanggaard and F. C. Krebs, *Sol. Energy Mater. Sol. Cells*, 2004, **83**, 125–146.

[166] D. Gust, T. A. Moore and A. L. Moore, *Acc. Chem. Res.*, 2009, **42**, 1890–1898.

[167] J. S. Lee, S. H. Lee, J. H. Kim and C. B. Park, *Lab Chip*, 2011, **11**, 2309–2311.

[168] N. Robertson, *Angew. Chem., Int. Ed.*, 2008, **47**, 1012–1014.

[169] D. Erickson, D. Sinton and D. Psaltis, *Nat. Photonics*, 2011, **5**, 583–590.

[170] F. Li, J. Zhuang, G. Jiang, H. Tang, A. Xia, L. Jiang, Y. Song, Y. Li and D. Zhu, *Chem. Mater.*, 2008, **20**, 1194–1196.

[171] A. Khetani, M. Laferrière, H. Anis and J. C. Scaiano, *J. Mater. Chem.*, 2008, **18**, 4769–4774.

[172] J. M. Pratt, *J. Chem. Soc.*, 1964, 5154–5160.

[173] A. Vogler, R. Hirschmann, H. Otto and H. Kunkely, *Ber. Bunsen-Ges. Phys. Chem.*, 1976, **80**, 420–424.

[174] I. Ahmad, W. Hussain and A. A. Fareedi, *J. Pharm. Biomed. Anal.*, 1992, **10**, 9–15.

[175] H. M. D. Bandara and S. C. Burdette, *Chem. Soc. Rev.*, 2012, **41**, 1809–1825.

[176] S. Kobayashi, H. Yokoyama and H. Kamei, *Chem. Phys. Lett.*, 1987, **138**, 333–338.

[177] M. Poprawa-Smoluch, J. Baggerman, H. Zhang, H. P. A. Maas, L. De Cola and A. M. Brouwer, *J. Phys. Chem. A*, 2006, **110**, 11926–11937.

[178] G. Gabor and E. Fischer, *J. Phys. Chem.*, 1971, **75**, 581–583.

[179] N. A. Wazzan, P. R. Richardson and A. C. Jones, *Photochem. Photobiol. Sci.*, 2010, **9**, 968–974.

[180] M. Schmidt, A. M. Cubillas, N. Taccardi, T. G. Euser, T. Cremer, F. Maier, H.-P. Steinrück, P. St. J. Russell, P. Wasserscheid and B. J. M. Etzold, *ChemCatChem*, 2013, **5**, 641–650.

[181] A. M. Cubillas, M. Schmidt, T. G. Euser, B. J. M. Etzold, N. Taccardi, S. Unterkofler, P. Wasserscheid and P. St. J. Russell, European Conference on Lasers and Electro-Optics (CLEO Europe 2013), Munich, Germany, 2013.

[182] H. J. H. Fenton, *J. Chem. Soc. Trans.*, 1894, **65**, 899–910.

[183] K. Wu, Y. Xie, J. Zhao and H. Hidaka, *J. Mol. Catal. A: Chem.*, 1999, **144**, 77–84.

[184] J. J. Pignatello, E. Oliveros and A. MacKay, *Crit. Rev. Environ. Sci. Technol.*, 2006, **36**, 1–84.

[185] M. Cheng, W. Ma, J. Li, Y. Huang, J. Zhao, Y. Xiang Wen and Y. Xu, *Environ. Sci. Technol.*, 2004, **38**, 1569–1575.

[186] S. Malato, P. Fernández-Ibáñez, M. I. Maldonado, J. Blanco and W. Gernjak, *Catal. Today*, 2009, **147**, 1–59.

[187] A. Amezcua-Correa, J. Yang, C. E. Finlayson, A. C. Peacock, J. R. Hayes, P. J. A. Sazio, J. J. Baumberg and S. M. Howdle, *Adv. Funct. Mater.*, 2007, **17**, 2024–2030.

[188] F. M. Cox, A. Argyros, M. C. J. Large and S. Kalluri, *Opt. Express*, 2007, **15**, 13675–13681.

[189] Y. Han, S. Tan, M. K. Khaing Oo, D. Pristinski, S. Sukhishvili and H. Du, *Adv. Mater.*, 2010, **22**, 2647–2651.

[190] M. K. K. Oo, Y. Han, R. Martini, S. Sukhishvili and H. Du, *Opt. Lett.*, 2009, **34**, 968–970.

[191] H. Yan, C. Gu, C. Yang, J. Liu, G. Jin, J. Zhang, L. Hou and Y. Yao, *Appl. Phys. Lett.*, 2006, **89**, 204101.

[192] A. Corma and P. Serna, *Science*, 2006, **313**, 332–334.

[193] R. F. Straub, R. D. Voyksner and J. T. Keever, *Anal. Chem.*, 1993, **65**, 2131–2136.

[194] A. Jess and P. Wasserscheid, *Chemical Technology – an integral textbook*, Wiley-VCH, Weinheim, Germany, 1st edn, 2013.

[195] K. Jähnisch, V. Hessel, H. Löwe and M. Baerns, *Angew. Chem., Int. Ed.*, 2004, **43**, 406–446.

[196] P. Watts and S. J. Haswell, *Chem. Soc. Rev.*, 2005, **34**, 235–246.

[197] E. E. Coyle and M. Oelgemöller, *Photochem. Photobiol. Sci.*, 2008, **7**, 1313–1322.

[198] N. V. Lavrik, L. T. Taylor and M. J. Sepaniak, *Anal. Chim. Acta*, 2011, **694**, 6–20.

[199] J. P. Kutter, *J. Chromatogr., A*, 2012, **1221**, 72–82.

[200] I. M. Lazar, P. Trisiripisal and H. A. Sarvaiya, *Anal. Chem.*, 2006, **78**, 5513–5524.

[201] C. Liu and X. Zhang, *J. Chromatogr., A*, 2007, **1139**, 191–198.